Geoscientific
Model Development

The CO5 configuration of the 7 km Atlantic Margin Model: large-scale biases and sensitivity to forcing, physics options and vertical resolution

Enda O'Dea[1], **Rachel Furner**[1], **Sarah Wakelin**[2], **John Siddorn**[1], **James While**[1], **Peter Sykes**[1], **Robert King**[1], **Jason Holt**[2], **and Helene Hewitt**[1]

[1]Met Office, Exeter, UK
[2]National Oceanography Centre, Liverpool, UK

Correspondence to: Enda O'Dea (enda.odea@metoffice.gov.uk)

Abstract. We describe the physical model component of the standard Coastal Ocean version 5 configuration (CO5) of the European north-west shelf (NWS). CO5 was developed jointly between the Met Office and the National Oceanography Centre. CO5 is designed with the seamless approach in mind, which allows for modelling of multiple timescales for a variety of applications from short-range ocean forecasting to climate projections. The configuration constitutes the basis of the latest update to the ocean and data assimilation components of the Met Office's operational Forecast Ocean Assimilation Model (FOAM) for the NWS. A 30.5-year non-assimilating control hindcast of CO5 was integrated from January 1981 to June 2012. Sensitivity simulations were conducted with reference to the control run. The control run is compared against a previous non-assimilating Proudman Oceanographic Laboratory Coastal Ocean Modelling System (POLCOMS) hindcast of the NWS. The CO5 control hindcast is shown to have much reduced biases compared to POLCOMS. Emphasis in the system description is weighted to updates in CO5 over previous versions. Updates include an increase in vertical resolution, a new vertical coordinate stretching function, the replacement of climatological riverine sources with the pan-European hydrological model E-HYPE, a new Baltic boundary condition and switching from directly imposed atmospheric model boundary fluxes to calculating the fluxes within the model using a bulk formula. Sensitivity tests of the updates are detailed with a view toward attributing observed changes in the new system from the previous system and suggesting future directions of research to further improve the system.

1 Introduction

The European north-west shelf (NWS) is an area of intense socioeconomic interest with a wide variety of dynamical regimes. It is a region that has been the subject of numerous research models over many years both domain-wide and focusing on smaller subregions. Research models and associated assimilation schemes for the region have matured into a number of operational systems. As part of the Copernicus Marine Environment Monitoring Service (CMEMS), an operational forecast system based on the Atlantic Margin Model (AMM) domain (O'Dea et al., 2012) has been developed to provide products for coastal modelling downstream users. The AMM term refers to the model domain rather than the full configuration for the NWS as implemented at the Met Office. It is the model domain of previous Met Office NWS configurations up to and including CO5, and it is shown in Fig. 1.

Complimentary to the forecast systems, CMEMS also make reanalysis products available to the end users. The reanalysis products not only provide end users with data from
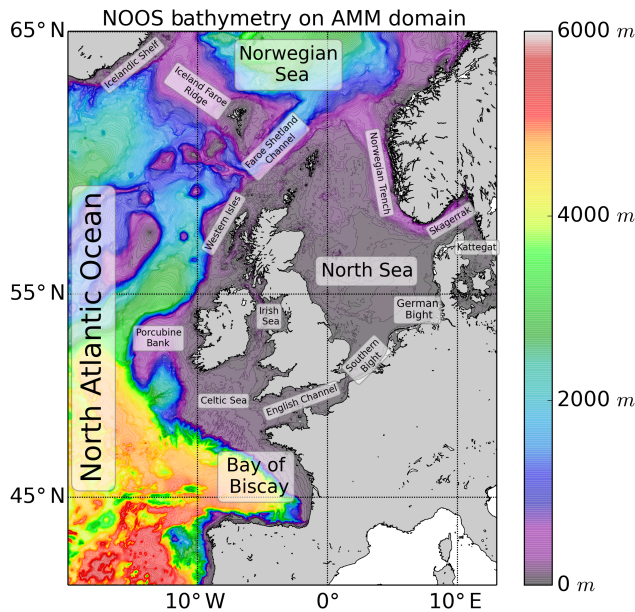
Figure 1. NOOS bathymetry for the AMM domain.

past decades but also provide a way to assess and validate the operational systems over longer periods against historical data. The presentation of systematic biases and drifts allows the users to understand the limitations and appropriateness of a particular product to their interest or application. Furthermore, as systems are upgraded, the associated reanalyses provide a means to intercompare and evaluate the effectiveness of system updates.

Here, we describe the non-assimilating standard Coastal Ocean configuration version 5 (CO5) control hindcast. This CO5 hindcast provides a reference to understand underlying biases and drifts attributable to changes in the physics updates alone. CO5 includes all input parameters, ancillary files, model code and compilation keys required to run the model. CO5 forms the physics component of the Copernicus reanalysis product replacing the preexisting POLCOMS-derived hindcast product. In support of the full reanalysis, a non-assimilative control hindcast was integrated from January 1981 to June 2012. CO5 was jointly developed by the Met Office and the National Oceanography Centre. Standard configurations such as CO5 are subsequently incorporated as constituent parts of broader modelling systems such as climate projections (Tinker et al., 2015) or coupled systems (Sikirić et al., 2013).

CO5 is an update of the Nucleus for European Modelling of the Ocean (NEMO) (Madec, 2008) configuration used to model the NWS in O'Dea et al. (2012). For convenience, we reference the configuration in O'Dea et al. (2012) as CO4. CO4 was also based on the operational AMM domain at the Met Office. Changes include new riverine forcing, updated Baltic boundary conditions, increased vertical resolution, different surface forcing, as well as an updated base NEMO

from version 3.2 to 3.4. The CO5 reanalysis product is an update to the 12 km POLCOMS hindcast (Holt et al., 2012) for 1965–2004 of the same AMM region. We compare the CO5 non-assimilative control hindcast with the POLCOMS hindcast over common years of integration for the period 1985–2004 and exclude the CO5 spin-up years 1981–1984. Both are compared against standard climatologies and observations. Individual updates incorporated into CO5 are also investigated systematically by a series of 30-year sensitivity experiments, looking at the changes in isolation. The surface and boundary forcing datasets used in CO4 only start from 2006, so it is not possible to do a full 30-year like-for-like CO4 and CO5 comparison. However, shorter 5-year experiments looking at the effects of the forcing are also investigated.

The structure of the paper is as follows. Section 2 gives an overview of the standard configuration CO5. Configuration updates are detailed in Sect. 3. The experimental design including the specifics of the sensitivity experiments are outlined in Sect. 4. Section 5 has three main subsections:

– Section 5.1 is concerned with tidal analysis of CO5.

– Section 5.2 isolates long-term biases compared to climatology, observations and the POLCOMS hindcast.

– Section 5.3 presents results from sensitivity experiments that look in isolation at changes brought into CO5.

Section 6 summarises and discusses the results before commenting on future system upgrades which are informed by the analysis of this paper.

2 Core model description

CO5 builds upon and thus shares many of the core features of the previous Met Office shelf seas model configuration CO4, as described in O'Dea et al. (2012). Elaboration of the key features particular to CO5 that are distinct from CO4 is deferred to Sect. 3.

CO5 is based on version 3.4 of NEMO (Madec, 2008). The model domain extends from 20° W, 40° N to 13° E, 65° N on a regular latitude–longitude grid. The domain covers the entirety of the European NWS and includes a sufficient portion of the deep waters of the eastern North Atlantic to encapsulate cross-shelf break exchange. The bathymetry for CO5 is derived from the North West European Shelf Operational Oceanographic System (NOOS) bathymetry. The NOOS bathymetry is a combination of GEBCO 1 arcmin data and a variety of local data sources from the NOOS partners. The meridional grid resolution is 1/15° or 7.4 km. The zonal resolution of 1/9° varies from 9.4 km along the southern boundary to 5.2 km along the northern boundary with a mean of 7.4 km at 52.5° N. Although the grid horizontal resolution readily resolves the external Rossby radius

(200 km), it is not sufficient to resolve the internal Rossby radius on the shelf which is of the order 4 km (Holt and Proctor, 2008). However, at the time of integration of the reanalysis, it was not computationally feasible to conduct multiple 30-year hindcasts of the CO5 domain with a resolution approaching the 1.5 km required to resolve the internal radius.

As tides and surges play such important roles on the European NWS, a non-linear free surface is implemented using the variable volume layer (Levier et al., 2007) and time-splitting approaches in NEMO. The baroclinic time step used in the 30-year hindcasts of CO5 is 300 s with a barotropic time step of 10 s. The advection of momentum is both energy and enstrophy conserving (Arakawa and Lamb, 1981). Both bi-Laplacian and Laplacian horizontal viscosities are applied. The Laplacian viscosity is applied along geopotential levels with a coefficient of $30.0\,\mathrm{m^2\,s^{-1}}$. The bi-Laplacian viscosity is used to retain model stability and is applied on model levels with a coefficient of $1.0 \times 10^{-10}\,\mathrm{m^4\,s^{-1}}$. The lateral momentum boundary condition is free slip. Tracer advection is implemented using the total variation diminishing (TVD) scheme (Zalesak, 1979). Unlike CO4, Laplacian tracer diffusion operates only along geopotential levels with a coefficient of $50\,\mathrm{m^2\,s^{-1}}$.

The generic length scale (GLS) turbulence scheme calculates the turbulent viscosities and diffusivities (Umlauf and Burchard, 2003). The second-moment algebraic closure of Canuto et al. (2001) is solved with two dynamical equations (Rodi, 1987) for the turbulence kinetic energy (TKE), k and TKE dissipation, ϵ (Umlauf and Burchard, 2005). At the surface and bed, Neumann boundary conditions on k and ϵ are applied. Surface wave mixing is parameterised as in Craig and Banner (1994). Dissipation under stable stratification is limited using the Galperin limit (Galperin et al., 1988) of 0.267. A spatially varying log-layer-derived drag coefficient with a minimum set at 0.0025 controls the bottom friction.

3 Summary of main model updates

CO5 has four configuration updates from CO4. These updates involve the vertical levels, the source riverine input, the treatment of the exchange with the Baltic through the Kattegat and the base version of NEMO. Furthermore, the inputs at the oceanic lateral boundary conditions and the surface boundary condition (SBC) for the 30-year hindcast are substantially different from the shorter runs detailed for the forecast implementation of CO4 in O'Dea et al. (2012). Here, we describe in detail each of the changes, and in Sect. 4 a set of sensitivity experiments explores the impacts of these changes.

3.1 Vertical coordinate

The vertical coordinate in CO5 is inherited from CO4 and is a $z^{*} - \sigma$ coordinate. It is terrain following and is fitted to a
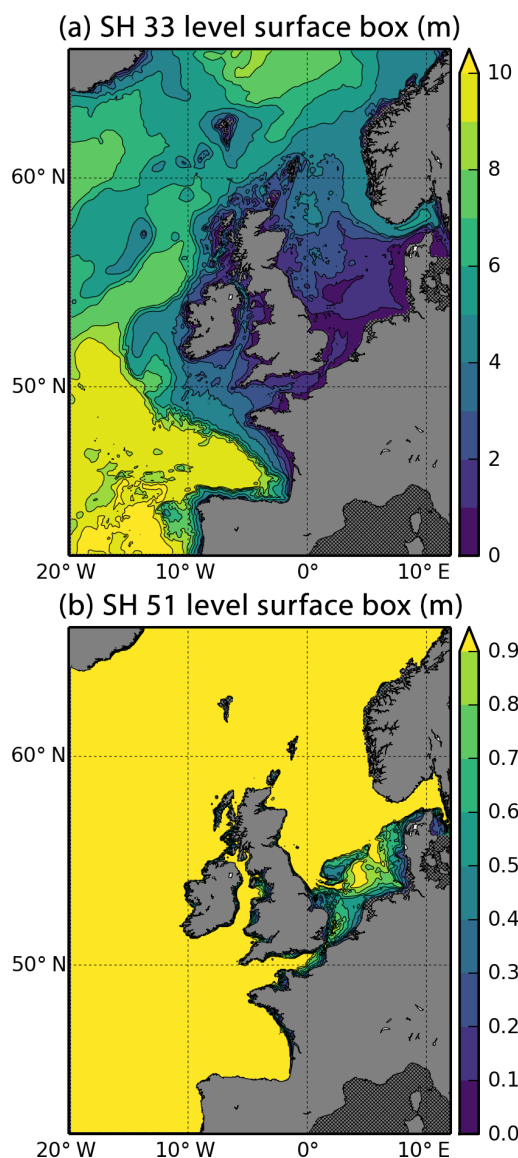

Figure 2. Thickness of surface model levels in CO4 (**a**) and CO5 (**b**).

smoothed envelope bathymetry. Where the actual bathymetry is too steep, it intersects the bed and levels are lost analogously to a z-level model. Relative to CO4, which uses the stretching function in Song and Haidvogel (1994), CO5 both features more model levels (increased from 33 to 51) and uses the stretching function as detailed in Siddorn and Furner (2013) for the terrain-following coordinate system. We refer to the stretching function in CO4 as SH and that in CO5 as SF. The new stretching function maintains near-uniform vertical resolution at the surface. Keeping the surface vertical resolution almost the same across most of the domain implies a more consistent air–sea exchange domain-wide. The stretching function also aims to minimise horizontal pressure gradient errors induced by sloping horizontal model levels.

A comparison of the thickness of the surface model level in CO4 and CO5 is shown in Fig. 2. It is only in the shallowest regions (bathymetry of less than 50 m) where the surface level thickness in CO5 is not set equal to 1 m, whereas in CO4 the surface model level varies considerably over the domain from deep water to shelf. Thus, any change in CO5 that impacts upon air–sea exchange will be applied equally across most of the domain allowing cause and effect to be more readily parsed. Furthermore, follow-on configurations of CO5 will feature ocean–atmosphere coupling where again consistent air–sea exchange will be important.

3.2 Riverine input

The second significant change between CO4 and CO5 is the data source for riverine input. In CO4, an annual climatology of some 320 European rivers mapped to 165 outflow points on the CO4 grid constitutes the riverine input regardless of the model year (Young and Holt, 2007). As a step towards temporal variation and higher resolution of riverine sources, the old climatology is replaced with data from a pan-European implementation of the hydrological model HYdrological Predictions for the Environment (HYPE) (Lindström et al., 2010). The European implementation of HYPE is known as E-HYPE (Donnelly et al., 2015) and has a sub-basin resolution of $120 \, \text{km}^2$. There is both an operational forecast and hindcast of E-HYPE, and the data are freely available at http://hypeweb.smhi.se/europehype/long-term-means. Daily river outflow data are mapped to 476 outflow points on the CO5 grid from version 2.1 of E-HYPE. Data were provided by the Swedish Meteorological and Hydrological Institute (SMHI) for the entire period of the hindcast. The E-HYPE data provide a greater number of river sources along the coastline of continental Europe. Figure 3 compares the total riverine input from all rivers in the domain for both the CO4 river climatology and the 1980–2012 mean of the E-HYPE data. Two individual years of E-HYPE data are also included to show the day-to-day and year-to-year variability that E-HYPE daily data contain compared to the climatological means. The difference in subregions along subsections of coast is shown in Fig. 4. The increase in continental river outflow leads to the mean E-HYPE outflow being considerably larger than the CO4 river climatology. However, as presented in Fig. 4, the increase is not uniform and indeed the mean outflow from regions of the UK is actually slightly reduced in E-HYPE. In some areas, such as the German Bight and the Norwegian coast, E-HYPE outflow is substantially increased.

3.3 Baltic exchange

The third update to CO5 concerns the exchange between the North Sea and the Baltic through the Danish straits and the Kattegat. At 7 km resolution, it is not possible to resolve the Danish straits, given that Öresund is 4 km wide at its narrow-
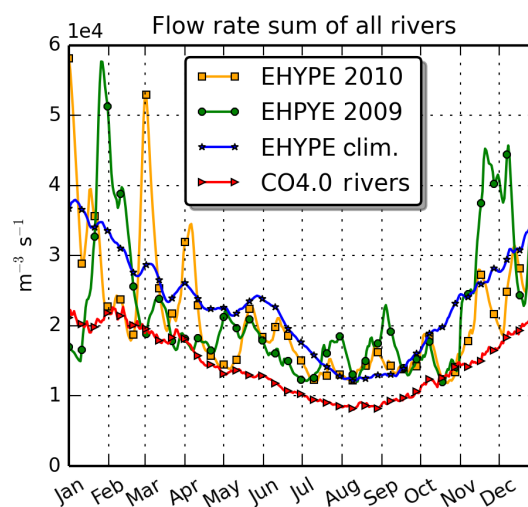

Figure 3. Comparison of total river flow rate between E-HYPE individual years, 30-year mean and CO4 climatological rivers.

est. Thus, alternative approaches are required. The approach in CO4 was to apply a daily climatological flux through two additional river points at roughly where the Great Belt and the Öresund open to the Kattegat. If the flux is negative, i.e. water leaves the Kattegat and enters the Baltic, ocean water is removed at the river point according to the magnitude of the flux. If the flux is positive, a flux of water of specified salinity and temperature is added at the river point. In CO5, a different approach is taken and involves the specification of a new lateral boundary condition with a relaxation zone spread across the Kattegat. No attempt is made to model the Danish straits and they are removed from the domain as seen in the hashed-out region of Fig. 2. Data for the lateral boundary condition come from a general estuarine transport model (GETM) of the North Sea and the Baltic Sea. The North Sea–Baltic Sea (NSBS) model was run at the Leibniz Institut für Ostseeforschung Warnemünde (IOW) (Gräwe et al., 2015). The horizontal resolution was 1 nautical mile, and there are 50 vertical levels. The version of GETM was v2.3.1. Daily NSBS data are only available from 2001 to 2012, and a climatology of this daily boundary dataset is created to cover 1981–2001. Temperature and salinity data are relaxed over the relaxation zone. Barotropic velocity and sea surface elevation boundaries from the NSBS model can also be prescribed by the Flather radiation boundary condition. However, the reference elevation in the NSBS model and the data from the models of the Atlantic into which CO5 is nested are not the same. Such a difference could lead to a persistent flux in or out of the Baltic that is not physically based. An anomaly of elevation about a mean value at the boundary could provide a suitable solution. For the hindcast, we describe here, only relaxation of the temperature and salinity is used, though a sensitivity run including elevation was conducted.
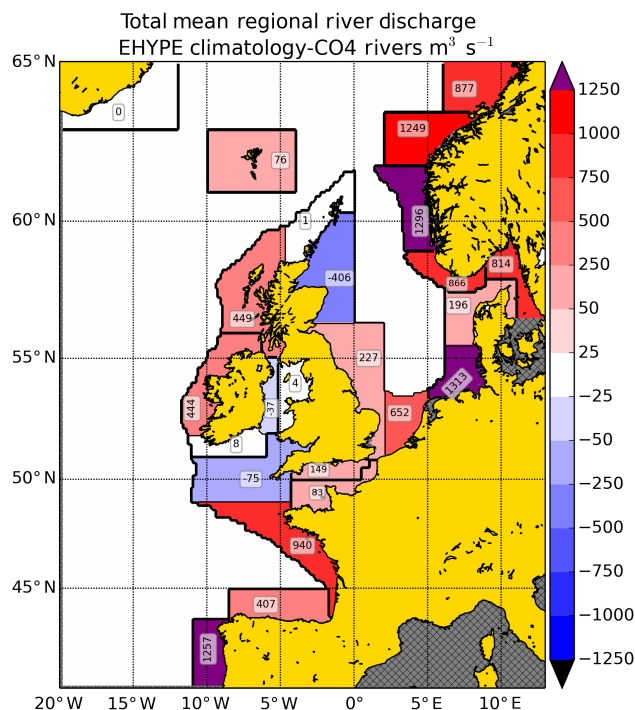
Total mean regional river discharge
EHYPE climatology-CO4 rivers m³ s⁻¹

Figure 4. Comparison of coastal subsections of total river flow rate between E-HYPE and CO4 climatological rivers.

3.4 Surface boundary condition

The surface boundary condition in CO5 has also changed from CO4. In CO4, the surface boundary conditions are directly prescribed fluxes from the Met Office's numerical weather prediction (NWP) model. Directly prescribed fluxes are replaced by calculating momentum, heat and freshwater fluxes using the Common Ocean-ice Reference Experiment (CORE) bulk formulae (Large and Yeager, 2009). The NWP data are only available from November 2006, and so a different surface boundary condition must be used for the 30-year CO5 hindcasts starting in 1981. The atmospheric forcing dataset used to force the 30-year hindcast is the ERA-Interim dataset of the European Centre for Medium-Range Weather Forecasts (ECMWF) (Dee et al., 2011). In addition to switching to bulk formulae, the light attenuation scheme used in CO5 is also changed to the standard NEMO tri-band red–blue–green (RGB) scheme of Lengaigne et al. (2007). The RGB scheme replaces the single-band scheme presented in Holt and James (2001) which is used in CO4. We refer to this single-band scheme as PDWL in this paper. One consequence of this change in the light scheme in CO5 is that the extinction depths do not vary across the domain in proportion to the bathymetry as in CO4 and POLCOMS. The variance in extinction depth was a first-order attempt to mimic the change in water clarity from deep waters to shallow.

4 Experimental design

The CO5 control run forms the baseline experiment for this paper. This baseline control run and the older POL-COMS hindcast are compared to evaluate how the two modelling systems perform irrespective of assimilation. The relevant configuration differences between CO5, CO4 and POL-COMS are shown in Table 1.

The configurations are compared with respect to satellite-derived sea surface temperature (SST), in situ subsurface observations, as well as both global and regional climatologies. To establish the effect of the key changes from CO4 to CO5, a set of sensitivity experiments are integrated over the full 30-year period. The key differences of the 30-year experiments are listed in Table 2.

The shorter CO4 experiments in O'Dea et al. (2012) used direct fluxes from NWP atmospheric forcing at v3.2 of NEMO. The Met Office NWP forcing dataset only covers November 2006–2012. Thus, to investigate the effect of the different surface forcing, a second set of experiments was integrated. The key differences are shown in Table 3.

This second set of experiments also determines the difference between upgrading the NEMO code and keeping all other parameters as similar as is feasible. In the CO4 experiments, there was also a bug involving the application of the inverse barometer at the lateral boundaries, and its effect is explored in the 5-year experiments by re-inclusion in one v3.4 experiment.

4.1 Model initialisation and forcing

CO5 was initialised in January 1981 by interpolating temperature and salinity fields from the 1/4° ORCA025 hindcast of the standard global ocean configuration GO5.0 (Megann et al., 2014). GO5.0 was itself initialised from a mean of the EN3 monthly objective analysis (Ingleby and Huddleston, 2007) and integrated from 1976 to 2005. The lateral open ocean boundary conditions for 1981 to 1989 were also taken from the GO5.0 hindcast. However, the boundary conditions from 1989 onwards were taken from the Global Seasonal Forecast system version 5 (GLOSEA5) (MacLachlan et al., 2015). GLOSEA5 was chosen for this period as it includes data assimilation. Unfortunately, there was no continuous run of GLOSEA5 that covered all of 1989–2012. Instead there were only two separate runs of GLOSEA5 available. The first GLOSEA5 run covered 1989–2003 and the second covered 2003–2012. The different global models all had different mean sea surface height (SSH) which needed to be matched as close as feasible to limit jumps at the cross-over dates. Furthermore, both the GO5.0 hindcast and the first 4 years of the GLOSEA5 integration have substantial drifts that needed to be removed. Details on the drift removal are given in Appendix B. From 1993 onwards, GLOSEA5 is constrained by assimilation of altimeter data, and no SSH drift removal is required over this period. NSBS GETM data

Table 1. Key configuration differences.

Configuration	POLCOMS	CO4	CO5
Code base	POLCOMS	NEMO 3.4	NEMO3.6
Horizontal resolution	12 km	7 km	7 km
Vertical levels	40 SH levels	33 SH levels	51 SF levels
Surface forcing	ERA40	NWP	ERAI
Lateral boundary	1°global	North Atlantic 12 km	1/4° global GO5.0 and GLOSEA5
River source	Climatology	Climatology	E-HYPE
Baltic boundary	Climatology at two points	Climatology at two points	IoW boundary condition
Light penetration	PDWL	PDWL	RGB
Integration period	1960–2004	2007–2012	1981–2012

NWP refers to Met Office numerical weather prediction (NWP) fluxes directly prescribed. IoW refers to data from the IoW NSBS GETM model of the Baltic (Gräwe et al., 2015). RGB is the default tri-band light attenuation scheme in NEMO (Lengaigne et al., 2007). PDWL refers to the single-band scheme that varies attenuation in proportion to sea bed depth (Holt and James, 2001).

Table 2. The 30-year sensitivity experiments.

EXP	Levels	River	Baltic	Light
CNTL	SF51	E-HYPE	IoW	RGB
S30_1	SH33	E-HYPE	IoW	RGB
S30_2	SH33	Climatology	Climatology	RGB
S30_3	SH33	Climatology	IoW	RGB
S30_4	SH33	E-HYPE	Climatology	RGB
S30_5	SF51	E-HYPE	IoW	PDWL

CNTL is the CO5 control. SF51 refers to 51 SF levels. SH33 refers to 33 SH levels. IoW refers to data from the IoW NSBS GETM model of the Baltic (Gräwe et al., 2015). RGB is the default tri-band light attenuation scheme in NEMO (Lengaigne et al., 2007). PDWL refers to the single-band scheme that varies attenuation in proportion to sea bed depth (Holt and James, 2001).

Table 3. The 5-year sensitivity experiments.

EXP	NEMO	Invbar	Boundary data	SBC
S5_1	v3.4	No	ORCA025	NWP
S5_2	v3.4	Yes	ORCA025	NWP
S5_3	v3.2	No	ORCA025	NWP
S5_4	v3.4	No	NATL12	NWP
S5_5	v3.4	No	ORCA025	ERAI

All 5-year experiments use the single-band light attenuation of Holt and James (2001). S5_1–S5_4 use directly specified fluxes from the Met Office NWP model. S5_5 uses ERA-Interim (ERAI) derived fluxes as in the CO5 control. Versions v3.2 and v3.4 refer to the base version of NEMO. Invbar specifies whether the inverse barometer effect is added at the boundary or not. ORCA025 and NATL12 refer to the source model data used for the open lateral boundary conditions.

at 1 nautical mile resolution were made available from IoW for the years 2000–2012. For years prior to this, an annual climatology was created based on the 2000–2012 NSBS GETM data. In the control run, river forcings from E-HYPE data are utilised for the full 30-year hindcast. The sensitivity experiments include hindcasts with the climatological rivers and climatological Baltic boundary to understand the impacts of the newer inputs.

Table 4. Elevation RMSE of amplitude in centimetres as compared to observations.

	M2	S2	K1	O1	N2
CO4	10.3	3.7	1.8	1.9	2.9
CO5	11.4	4.5	2.0	1.9	3.4
CO5*	9.5	4.0	1.8	1.6	3.3

CO5* refers to CO5 with lower reference density and time-splitting bug fix.

5 Results

5.1 Tidal harmonics

The co-tidal charts of the M2 SSH tidal harmonic, as analysed from CO4 and CO5, are given in Fig. 5. Overall, the general representation is fairly similar. CO4 and CO5 broadly agree with amphidrome positions derived from observations such as in Howarth and Pugh (1983). Whilst the position of degenerate amphidrome in southern Norway in CO5 may appear to align more closely with the observations, it must be noted that the data sparsity in this region is significant, and thus there is large uncertainty in the location of the degenerate amphidrome. In any case, it is found that the change in the land–sea mask from CO4 to CO5 due to the new Baltic boundary condition is the main driver behind the shift in the amphidrome rather than a targeted model improvement for the amphidrome's position. Two almost identical integrations of CO5 with and without the Baltic boundary masking were integrated. In the integration with the CO4 mask, the amphidrome returns to the position calculated in CO4.

Harmonic analysis of CO5 surface elevation is compared against tide gauge and bottom pressure data from the British Oceanographic Data Centre (BODC). Root mean square errors (RMSEs) of model SSH amplitude and phase are shown in Tables 4 and 5.

	M2	S2	K1	O1	N2
CO4	14.7	12.8	17.1	15.7	21.6
CO5	15.5	15.1	18.7	14.7	20.6
CO5*	12.6	11.8	15.4	14.8	19.2

CO5* refers to CO5 with lower reference density and time-splitting bug fix.

The CO5 configuration, as used in all sensitivity experiments in this paper, has a slightly larger RMSE in both amplitude and phase compared to CO4. Two issues behind this increase in error were found. One was due to an order of calculation bug in the time splitting in CO5. This resulted in a small error in the surface pressure gradient term. The second was in relation to the reference density within NEMO. In the CO4 configuration, the reference density was $1027\,\mathrm{kg\,m^{-3}}$. However, in CO5, the NEMO v3.4 default of $1035\,\mathrm{kg\,m^{-3}}$ was used. When these were corrected for, CO5 slightly improves upon CO4 when compared to the standard observations. To understand if these changes have any significant impact on the control and reanalysis, a further experiment with the changes was integrated. No significant difference in mean temperature or salinity fields was found.

5.2 Surface biases

5.2.1 Seasonal SST biases

The mean seasonal model SST from 1985 to 2004 is compared with remotely sensed products. These include the National Oceanic and Atmospheric Administration (NOAA) Advanced Very High Resolution Radiometer (AVHRR) product (Casey et al., 2010) and the European Space Agency (ESA) Climate Change Initiative (CCI) product (Merchant et al., 2014). The period 1985–2004 is chosen for two reasons. First, it allows for the CO5 hindcast to be spun up from rest in 1981. Secondly, it presents a common period with which to compare the POLCOMS hindcast that ends in 2005.

Figure 6 compares the CO5 control and POLCOMS hindcast SST bias against the AVHRR data. The largest bias in CO5 SST is the cold bias extending from eastern Iceland south-eastwards to the Faroe–Shetland Channel (FSC) and from the FSC north-westwards to the northern boundary of the domain. This SST bias is less apparent in summer as seen in Fig. 6c. The reduction in the bias might be caused by over-stratification in summer. The regions immediately surrounding the cold bias area appear to be warm biased in summer. This suggests the cold bias may be of a remote origin such as the boundary condition. Elsewhere off shelf there is a smaller cold bias in winter, spring and autumn. Along the Celtic shelf break, there is a slight warm bias. The model is probably underestimating the cold water surface signal associated with

enhanced vertical mixing at the shelf break. In summer, off shelf southward of 50° N, CO5 appears to be too warm. On shelf, CO5 SST is slightly cold biased in most regions for most seasons.

However, there are some warm biases, particularly in summer. The Southern Bight, the Western Isles of Scotland and the western Irish Sea all have summertime warm biases. The English Channel also has a warm SST bias in autumn.

Figure 6e–h show the equivalent seasonal SST bias for the POLCOMS hindcast. POLCOMS also has a large cold bias from Iceland to the FSC and from the FSC to the northern boundary in winter, spring and to some extent in autumn. However, the POLCOMS SST cold bias appears to be more extensive. It also extends south-westwards from the FSC to roughly the Porcupine Bank. Near the western boundary, there is also a significant warm SST bias in POLCOMS north of 55° N in winter. Off shelf in summer, there is a large warm bias in POLCOMS across much of the domain. However, there is also a large summertime SST cold bias in the Norwegian Trench, the Skagerrak and the Kattegat.

In summary, the CO5 control hindcast appears to have a much smaller SST bias than the preceding POLCOMS hindcast. One particularly large bias in CO5 is the large cold bias in the northern part of the domain which is also present in POLCOMS. This bias is explored further with comparisons against temperature and salinity profiles, as well as climatology. CO5 does appear to be too warm off shelf in summer but much less so than POLCOMS. On shelf, CO5 is generally slightly cold biased, whereas POLCOMS alternates from a large wintertime cold bias to a large summertime warm bias. POLCOMS is too cold in the Norwegian Trench during summer, while CO5 appears to do reasonably well there.

5.2.2 Surface salinity biases

The mean sea surface salinity (SSS) of CO5 for 1985–2004 and the POLCOMS hindcast are compared against the World Ocean Atlas 2013 (WOA13) global climatology (Zweng et al., 2013), the KLIWAS North Sea climatology (KLIWAS) (Bersch et al., 2013) and EN4 (Good et al., 2013) profile data in Fig. 7. A similar pattern in negative SSS bias as SST bias from Iceland to the FSC and to the northern boundary is present in CO5. With the exception of this northern region, CO5 off shelf is in reasonably good agreement with both the climatology and the mean profiles. However, POLCOMS appears too fresh off shelf except along the western French coast, indicating an offset in surface salinity between CO5 and POLCOMS. On the shelf, CO5 is in general slightly too saline. In particular, the Irish Sea is saline biased in CO5 and indicates the E-HYPE freshwater flux may be too small there.

Both CO5 and POLCOMS have large SSS biases compared to the climatologies and profiles in the Norwegian Trench. POLCOMS is too saline in the Norwegian Trench, while the salinity bias in CO5 is a dipole: near the Norwe-
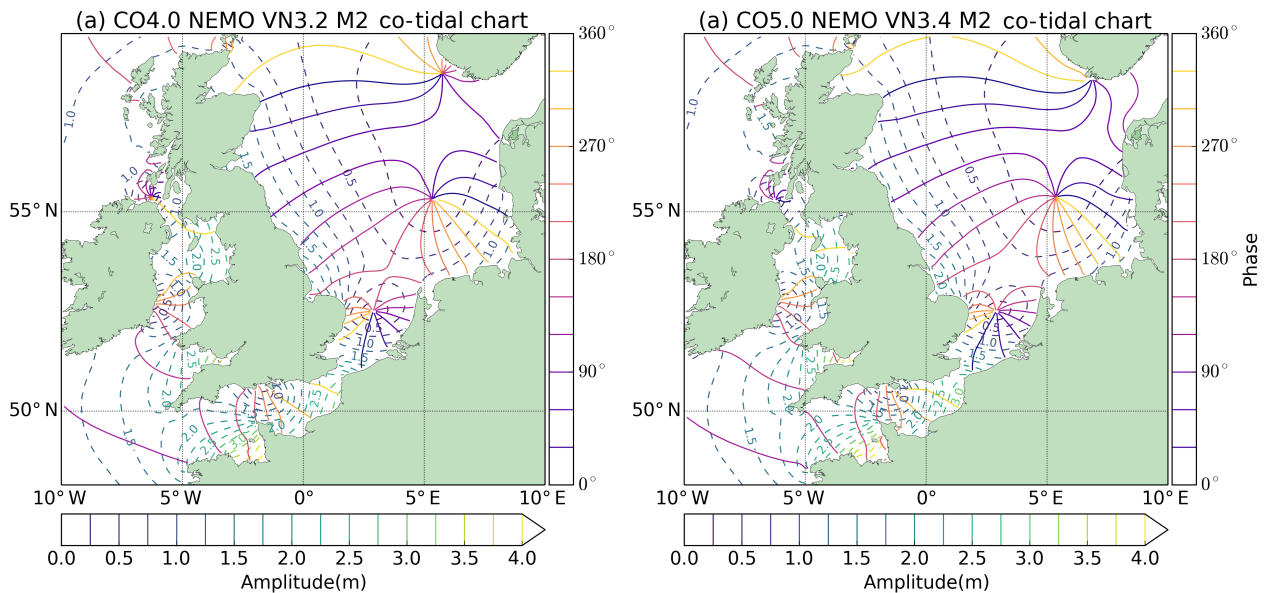
Figure 5. M2 co-tidal charts. **(a)** CO4, NEMO v3.2. **(b)** CO5, NEMO v3.4.
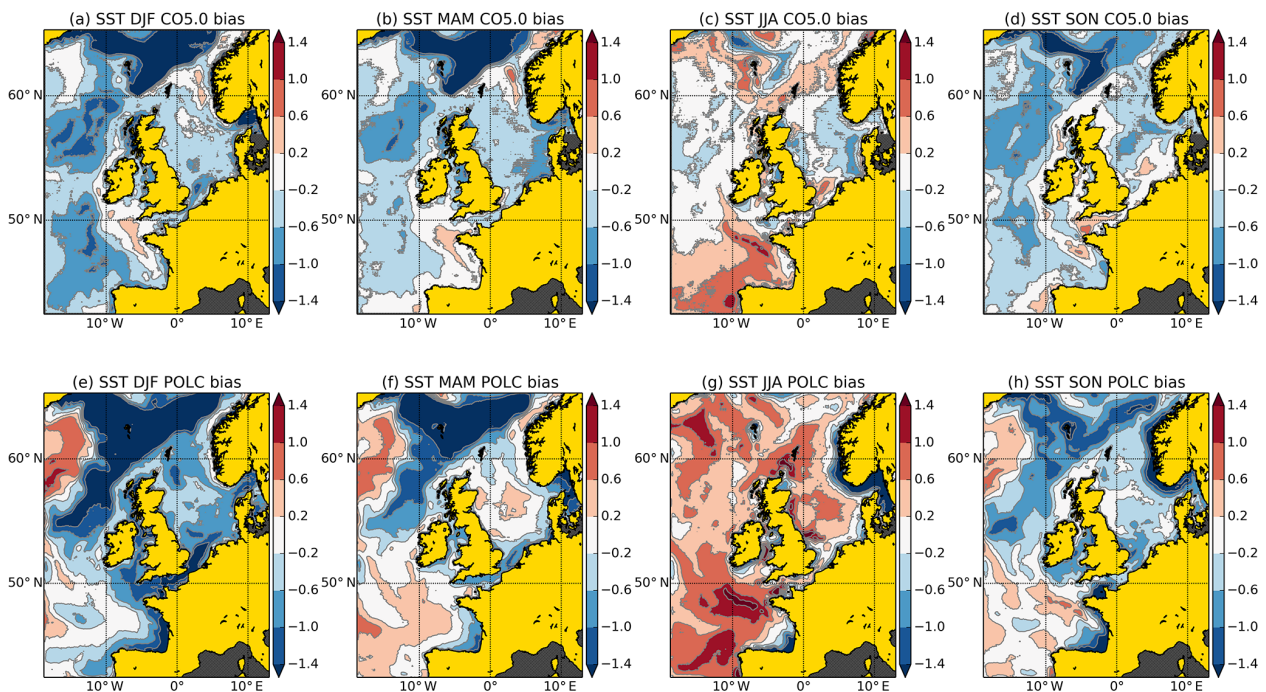

Figure 6. The difference between the mean seasonal model SST and the mean satellite SST for 1985–2004. **(a)** CO5 December–January–February (DJF) bias, **(b)** CO5 spring March–April–May (MAM) bias, **(c)** CO5 summer June–July–August (JJA) bias, **(d)** CO5 autumn bias September–October–November (SON), **(e)** POLCOMS (POLC) winter (DJF) bias, **(f)** POLC spring (MAM) bias, **(g)** POLC summer (JJA) bias and **(h)** POLC autumn bias (SON).

gian coast it is too fresh and near the western limb of the Norwegian Trench it is too saline. In POLCOMS, not only are there fewer vertical levels but the vertical resolution near the surface is proportional to the ocean depth as in CO4. Consequently, compared to CO5, the surface resolution in POL-

COMS in the Norwegian Trench is much reduced. The surface resolution in POLCOMS over the Norwegian Trench is typically 4 to 5 m compared to the uniform 1 m resolution for CO5. This may account for the much more saline SSS in POLCOMS there. The Baltic boundary in POLCOMS is
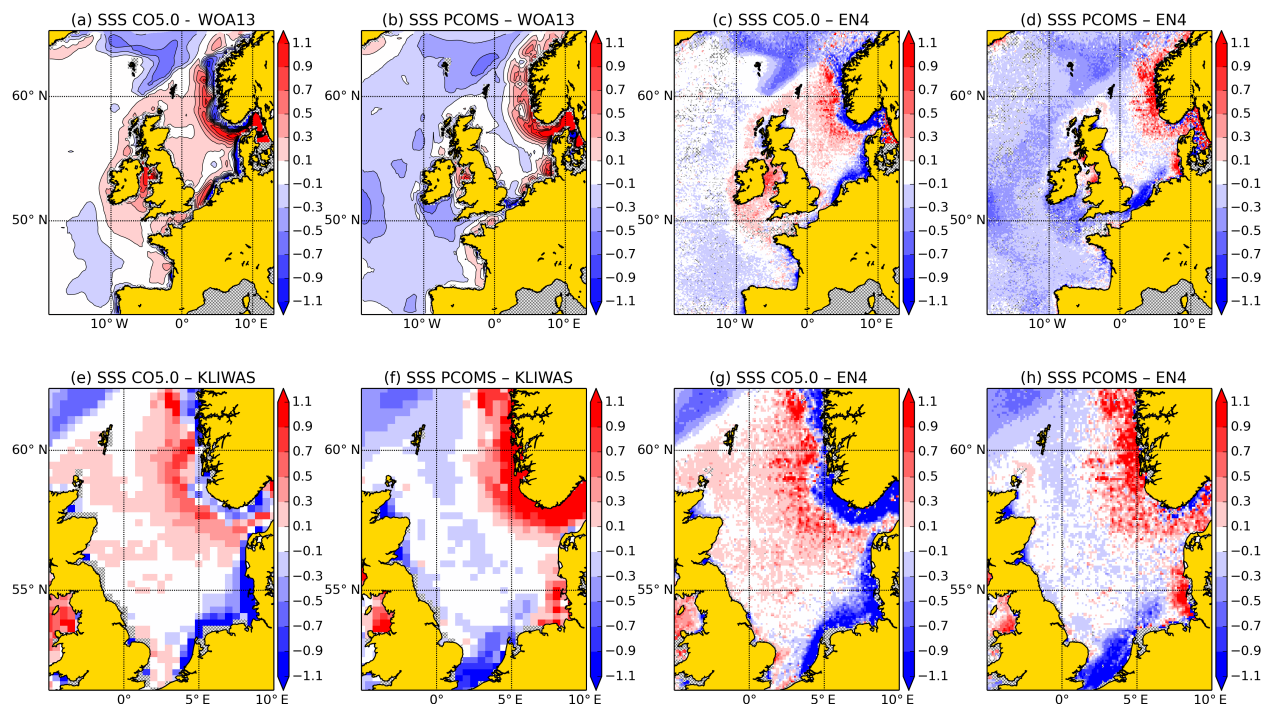
Figure 7. Mean model sea surface salinity (SSS) differences 1985–2004 from WOA13, KLIWAS and EN4: **(a)** CO5 – WOA13 climatology, **(b)** POLCOMS – WOA13 climatology, **(c)** O5 – EN4, **(d)** POLCOMS – EN4, **(e)** CO5 – KLIWAS North Sea climatology, **(f)** POLCOMS – KLIWAS North Sea climatology, **(g)** CO5 – EN4 in the North Sea and **(h)** POLCOMS – EN4 in the North Sea.

also more similar to CO4 than CO5 when using climatological river points to represent the exchange with the Baltic. The sensitivity experiments below investigate the effect of both these changes within the NEMO framework. With regards to the dipole in CO5, the resolution at 7 km is not sufficient to resolve the intense mixing processes in the trench where northward-flowing freshwater of Baltic origin along the Norwegian coast mixes laterally with adjacent incoming southward-flowing saline Atlantic water. It is anticipated that with increased horizontal resolution, better representation of eddy-induced mixing may reduce the dipole there.

POLCOMS and CO5 have biases of opposite signs in the German Bight; CO5 is too fresh and POLCOMS is too saline. POLCOMS uses the climatological rivers as in CO4 in contrast to the E-HYPE rivers used in CO5. Thus, the sensitivity experiments S30_1, S30_2 and S30_3 that compare the different river sources should help to understand the difference in this bias. POLCOMS also appears to be too fresh in the Southern Bight, and this may be contributing to the saline bias in the German Bight. POLCOMS may not be advecting the Rhine outflow to the east close enough to the coast. CO5 in contrast appears to be too fresh in the vicinity of the Rhine outflow.

5.2.3 Off-shelf temperature and salinity biases through depth against WOA13 climatology

To assess how CO5 and POLCOMS behave throughout the water column off shelf, they are compared against WOA13 data. Figure 8 displays both zonal transects and depth level temperature biases for 1985–2004 compared to WOA13. Both CO5 and POLCOMS temperature biases are included in Fig. 8. Figure 9 is the equivalent salinity plot. As the mean is for the entire period, seasonal biases such as in the SST plots of Fig. 6 are not discernible. The location of the transects are chosen to intersect regions of particularly large bias. Note that these comparisons use the CMEMS POLCOMS dataset, which was interpolated onto standard depth levels from the native POLCOMS grid which uses 40 s levels in the vertical (Holt et al., 2012). The interpolated POLCOMS data are particularly coarse at depth which is reflected in the step-like nature of the POLCOMS bias plots at depth. This accounts for some of the differences seen towards the bottom of profiles in Fig. 8.

In Fig. 8, the first two columns are zonal transects of difference in the mean temperature from the WOA13 climatology over the period 1985–2005. The first column is for CO5 and the second POLCOMS. The geographical extent of the biases highlighted in the transects is shown for four depths in the last two columns of Fig. 8. Both CO5 and POLCOMS have a cold water bias centred around roughly 1000 m that orig-
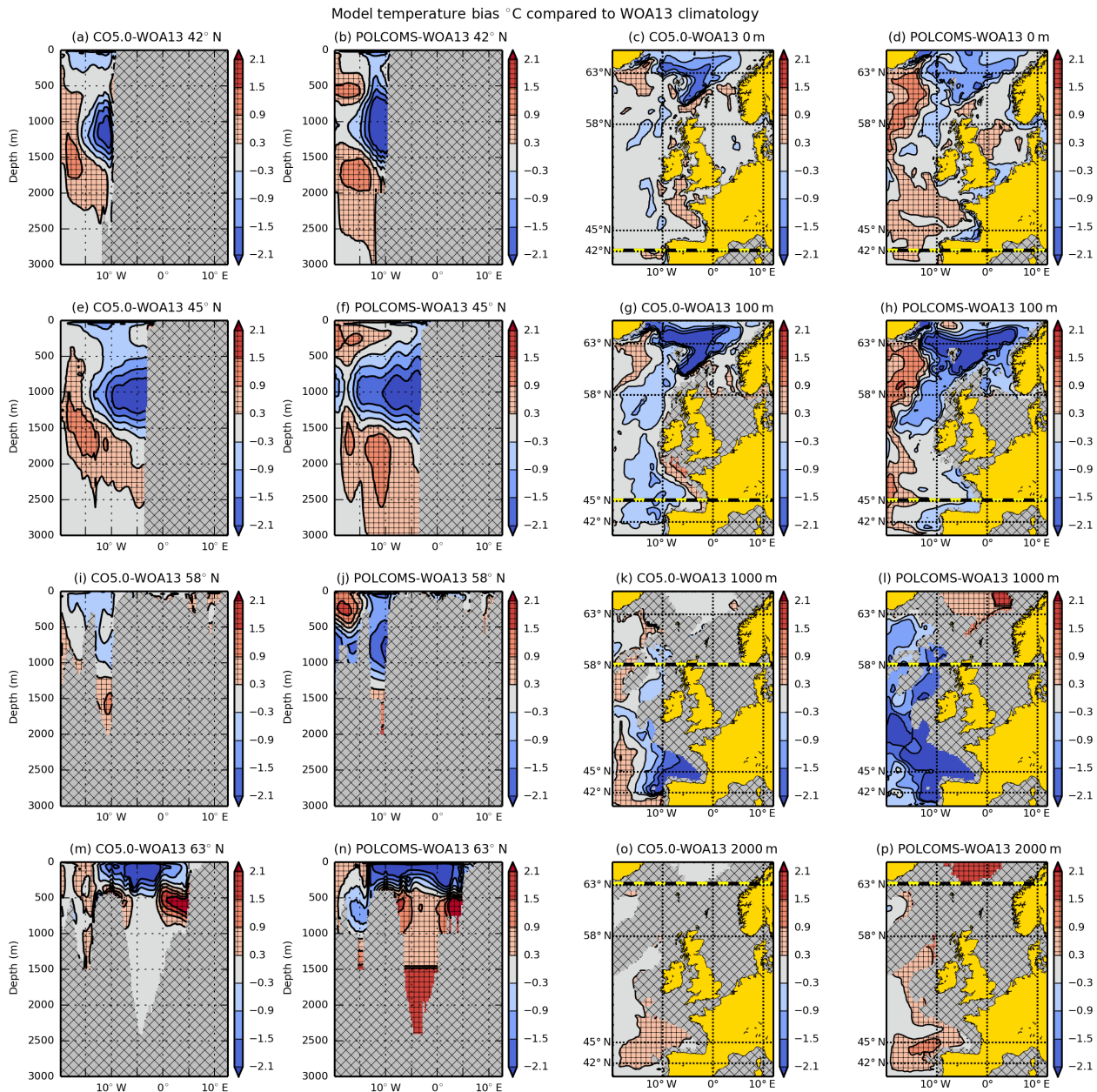
Model temperature bias °C compared to WOA13 climatology

Figure 8. CO5 and POLCOMS temperature bias compared to WOA13 1985–2005. Panels **(a)**, **(e)**, **(i)** and **(m)** are CO5 – WOA13 temperature bias transects along 42, 45, 58 and 63° N. Panels **(b)**, **(f)**, **(j)** and **(n)** are POLCOMS – WOA13 temperature bias transects along 42, 45, 58 and 63° N. Panels **(c)**, **(g)**, **(k)** and **(o)** are the CO5 – WOA13 temperature bias at depths 0, 100, 1000 and 2000 m. Panels **(d)**, **(h)**, **(l)** and **(p)** are the POLCOMS – WOA13 temperature bias at depths 0, 100, 1000 and 2000 m.

inates near the southern boundary away from the relaxation zone. A warm temperature bias surrounds the cold temperature bias away from the coast. A similar pattern in salinity bias is shown in Fig. 9. It appears the models are diffusing both horizontally and vertically the warm and saline waters of Mediterranean origin entering the domain from the southern boundary. The extra diffusion in the relaxation zone and the relatively coarse vertical resolution of about 100 m at a depth of 1000 m may be contributing to the loss in identity of

the Mediterranean waters. The anomaly is also present in the Bay of Biscay but is much reduced in CO5 further north.

In the seasonal SST anomalies, a large cold bias was shown in both CO5 and POLCOMS in winter. This cold bias is also present with respect to the WOA13 climatology. In CO5 and POLCOMS, it extends down to around 500 m. There is a warm bias in CO5 along the sea bed of the Iceland–Faroe ridge at around 500 m and at a similar depth on the Shetland side of the FSC. The vertical resolution of POL-

COMS is quite coarse at this depth. However, it suggests that at depths greater than 500 m POLCOMS is warm biased in the FSC and Norwegian Sea, and CO5 appears to be close to the climatology below 500 m. There is a similar pattern in the salinity bias with both CO5 and POLCOMS relatively fresh near the surface in this region. On the other hand, POLCOMS appears to be slightly fresher than WOA13 off shelf right through depth for most of the domain. Off shelf, away from Biscay and the northern boundary, CO5 salinity is quite similar to WOA13.

5.2.4 North Sea temperature and salinity biases through depth

The KLIWAS climatology for the NWS in combination with EN4 provides an alternative to WOA13 for evaluation of the models on the shelf itself. Figures 10 and 11 compare CO5 with both the KLIWAS climatology and the EN4 data over the period 1985–2004. A comparison of POLCOMS against KLIWAS is also included as a reference. Figure 10 focuses on the summer months when there is seasonal thermal stratification, while Fig. 11 is the salinity mean for all seasons. Including all seasons allows for a larger number of in situ profiles to compare against. In addition to biases at depth levels of 10, 30 and 40 m, transects are taken through areas of significant bias to give an overview of the vertical structure in the model bias.

Generally, the structure of the temperature bias between CO5 and EN4 is in reasonable agreement with the structure of the bias between CO5 and the KLIWAS climatology. In the seasonally stratified areas of the North Sea, CO5 compares favourably near the surface compared to POLCOMS. POLCOMS there is significantly warm biased. Immediately below the thermocline, both CO5 and POLCOMS are cold biased with the cold bias in POLCOMS being somewhat larger than CO5. In CO5, the cold bias does not extend to the bed and in fact reverses sign to be warm biased near the bed, whilst in POLCOMS the cold bias reduces towards the bed with only a small bias remaining at the sea floor. The light attenuation schemes in CO5 and POLCOMS are quite different and may partially explain why POLCOMS is more warm biased at the surface and more cold biased at depth. The light scheme used in POLCOMS (PDWL) is also implemented in CO4 and is included in the sensitivity experiments to enable its impact to be assessed.

The CO5 salinity bias against EN4 is also broadly in agreement with the bias against the KLIWAS climatology. As in the surface plots of Fig. 7, over most of the North Sea, CO5 is slightly too saline through depth. Along the coasts of Holland, Germany and Denmark, CO5 is clearly too fresh, suggesting too much riverine input as discussed earlier. Away from the coasts, POLCOMS is in fairly good agreement with EN4 and KLIWAS while just slightly fresher at depth. The transects in Fig. 11 are taken to go through the Norwegian Trench and the Rhine plume. CO5 is shown to be roughly 0.5

too fresh above 20 m in the Norwegian Trench near the coast of Norway, while below 20 m CO5 is slightly too saline. The warmer and more saline water from the Atlantic appears to make CO5 too saline along the rim of the Norwegian Trench. In contrast, POLCOMS is shown to be typically greater than 1.1 too saline above 20 m in the Norwegian Trench, while below 40 m, POLCOMS switches from the large saline bias to a significantly fresh bias. It appears that CO5 is representing the haline stratification in the Norwegian Trench with greater fidelity than POLCOMS. Both the vertical resolution and the Baltic boundary condition may play some role in this and are included in the sensitivity experiments that follow.

5.3 The 30-year sensitivity runs

5.3.1 Vertical levels and stretching function

The effect of the changes of surface vertical resolution between CO4 and CO5 is shown in Fig. 2. Sensitivity experiment S30_1 is exactly the same as the control (CNTL) except it uses 33 SH vertical levels instead of 51 SF levels. Although there are some small changes in summertime stratification off the shelf, the most dramatic change concerns the surface salinity in the Norwegian Trench. Figure 12 is the difference in salinity at 5 m between the control experiment CNTL (SF51) and sensitivity experiment S30_1 (SH33). The extra vertical resolution in the control run results in less diffusion of the surface fresh layer with depth. The POLCOMS hindcast also has much less vertical resolution at the surface than CO5, which may be one factor underlying its saline bias in the surface waters of the Norwegian Trench.

5.3.2 Baltic and rivers

Both the river forcing and Baltic boundary condition are changed in CO5 from climatological inputs to E-HYPE riverine inputs and IoW Baltic boundary data. The 30-year sensitivity experiments S30_2 and S30_1 are compared in Fig. 13. S30_1 is a 33-level version of the CO5 control but with exactly the same E-HYPE rivers and IoW Baltic boundary. S30_2 is exactly the same as S30_1 except that it uses the older climatological inputs for rivers and Baltic boundary as used in CO4. Figure 13a shows the surface salinity bias against EN4 data for S30_1. Figure 13b is the same but for S30_2 and shows a large reduction in the freshwater bias in the German Bight. Figure 13c compares experiment S30_3 with S30_1 to show differences created by the change in rivers alone. For most of continental Europe, the E-HYPE rivers clearly have a greater discharge as shown in Fig. 4. The difference is pronounced in the German Bight and along the Norwegian coast and is likely contributing to the fresh bias in CO5 compared to EN4 data there. Another possible source of salinity bias could be incorrect transports and representation of the North Sea circulation. Figure 14 shows a background field of mean transport in the North Sea and also
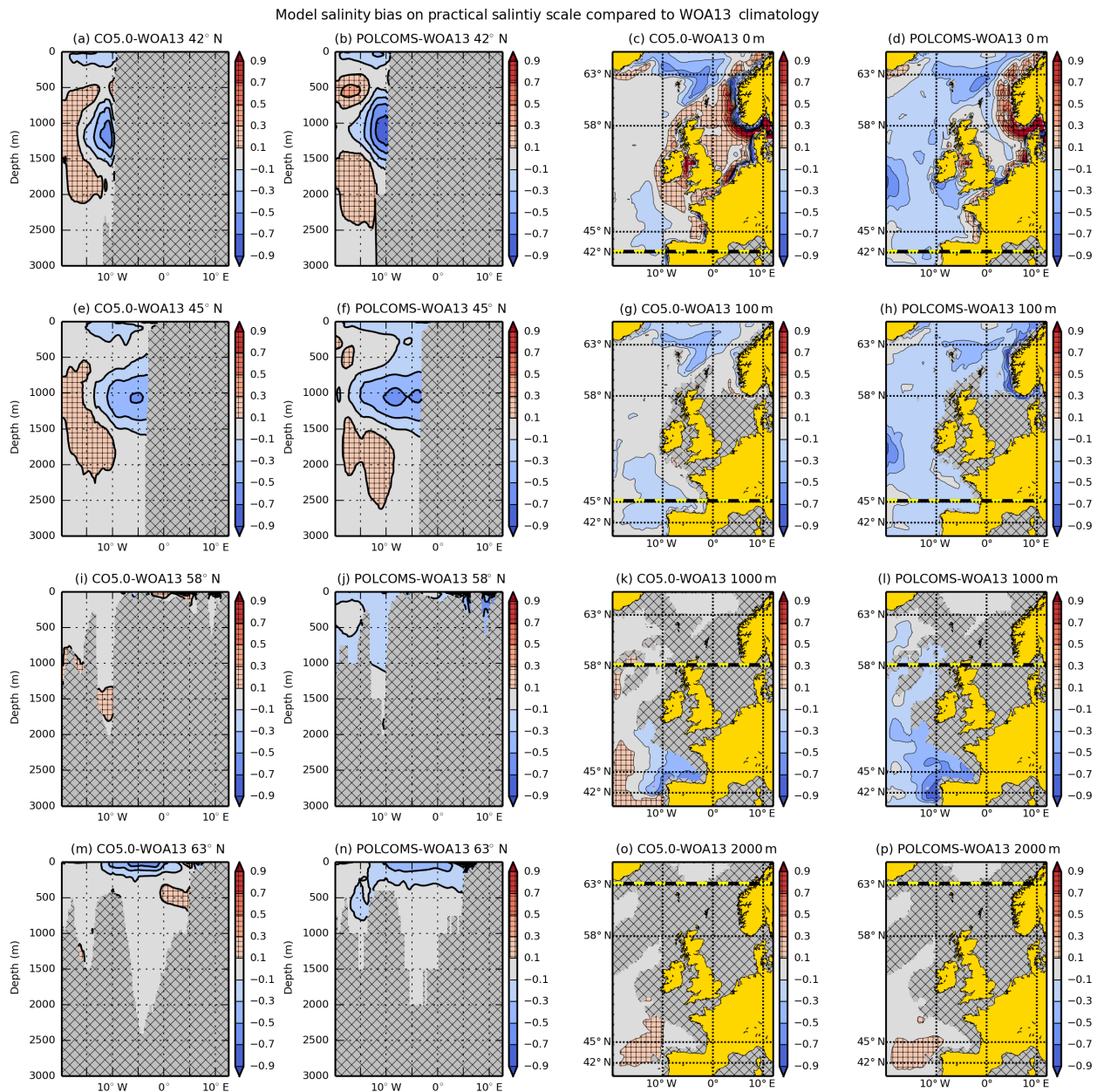
Figure 9. CO5 and POLCOMS salinity bias compared to WOA13 for 1985–2005. Panels **(a)**, **(e)**, **(i)** and **(m)** are CO5 – WOA13 salinity bias transects along 42, 45, 58 and 63° N. Panels **(b)**, **(f)**, **(j)** and **(n)** are POLCOMS – WOA13 salinity bias transects along 42, 45, 58 and 63° N. Panels **(c)**, **(g)**, **(k)** and **(o)** are the CO5 – WOA13 salinity bias at depths 0, 100, 1000 and 2000 m. Panels **(d)**, **(h)**, **(l)** and **(p)** are the POLCOMS – WOA13 salinity bias at depths 0, 100, 1000 and 2000 m.

the mean transport across selected NOOS transects into and out of the North Sea. The calculated transports are similar to reported values from observational estimates as shown in Table 6.

Around parts of the coast of the UK, the E-HYPE river discharge in some regions is actually slightly less than the climatology or only slightly greater in others. This is also reflected in the difference of salinity shown in Fig. 13c. Combining the correlation between areas of larger E-HYPE river

discharge than climatological rivers and the larger salinity biases in CO5 with what appears reasonable transports in CO5, it seems likely that the E-HYPE rivers are the first-order source of the salinity biases observed in CO5.

Figure 13d compares experiment S30_4 with S30_1 to show the impact resulting from the different Baltic boundaries. The IoW boundary results in a slightly more saline SSS over in the Norwegian Trench. The effect of the Baltic boundary condition is much smaller than the freshening due
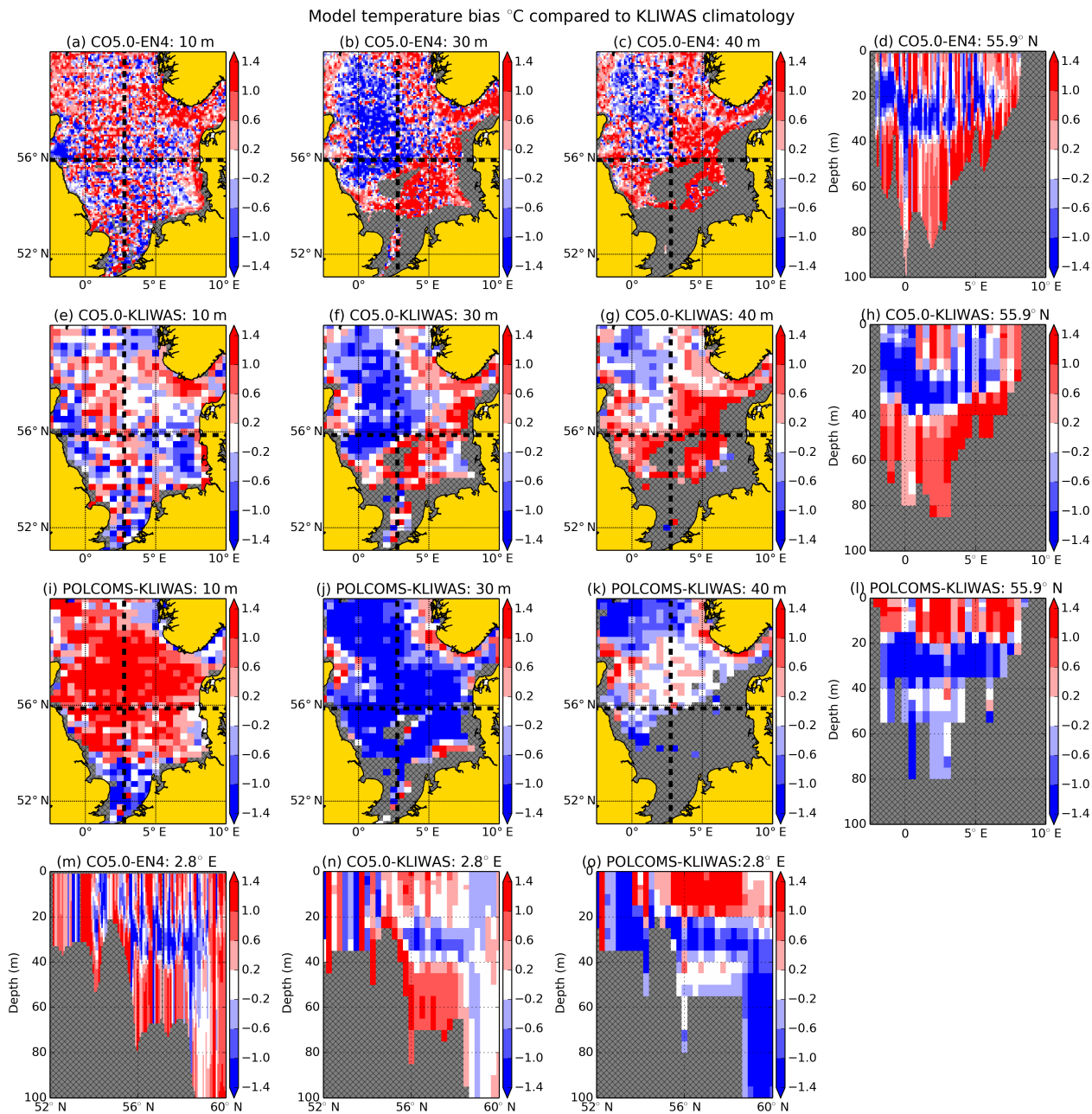
Figure 10. North Sea temperature bias compared to EN4 and the KLIWAS climatology for summer (JJA). Panels **(a)**–**(d)** compare CO5 and EN4 at 10, 30 and 40 m and along a transect at 56° N. Panels **(e)**–**(h)** compare CO5 and KLIWAS climatology at 10, 30 and 40 m and along a transect at 56° N. Panels **(e)**–**(h)** compare POLCOMS and KLIWAS climatology at 10, 30 and 40 m and along a transect at 56° N. Panels **(m)**–**(o)** are transects through depth for each case along longitude 2.8° E.

Table 6. Net transports across NOOS sections.

Name	NOOS ID	Paper reference	Observational value	CO5 value
Feie–Shetland west	1	Otto et al. (1990)	0.6 Sv	0.54 Sv
Feie–Shetland east	2	Otto et al. (1990)	0.7–1.1 Sv	1.11 Sv
Orkney–Shetland	3	Otto et al. (1990)	0.3 Sv	0.4 Sv
Dover Strait	13	Prandle et al. (1996)	0.09 Sv	0.091 Sv

Model salinity bias on practical salinity scale compared to KLIWAS climatology
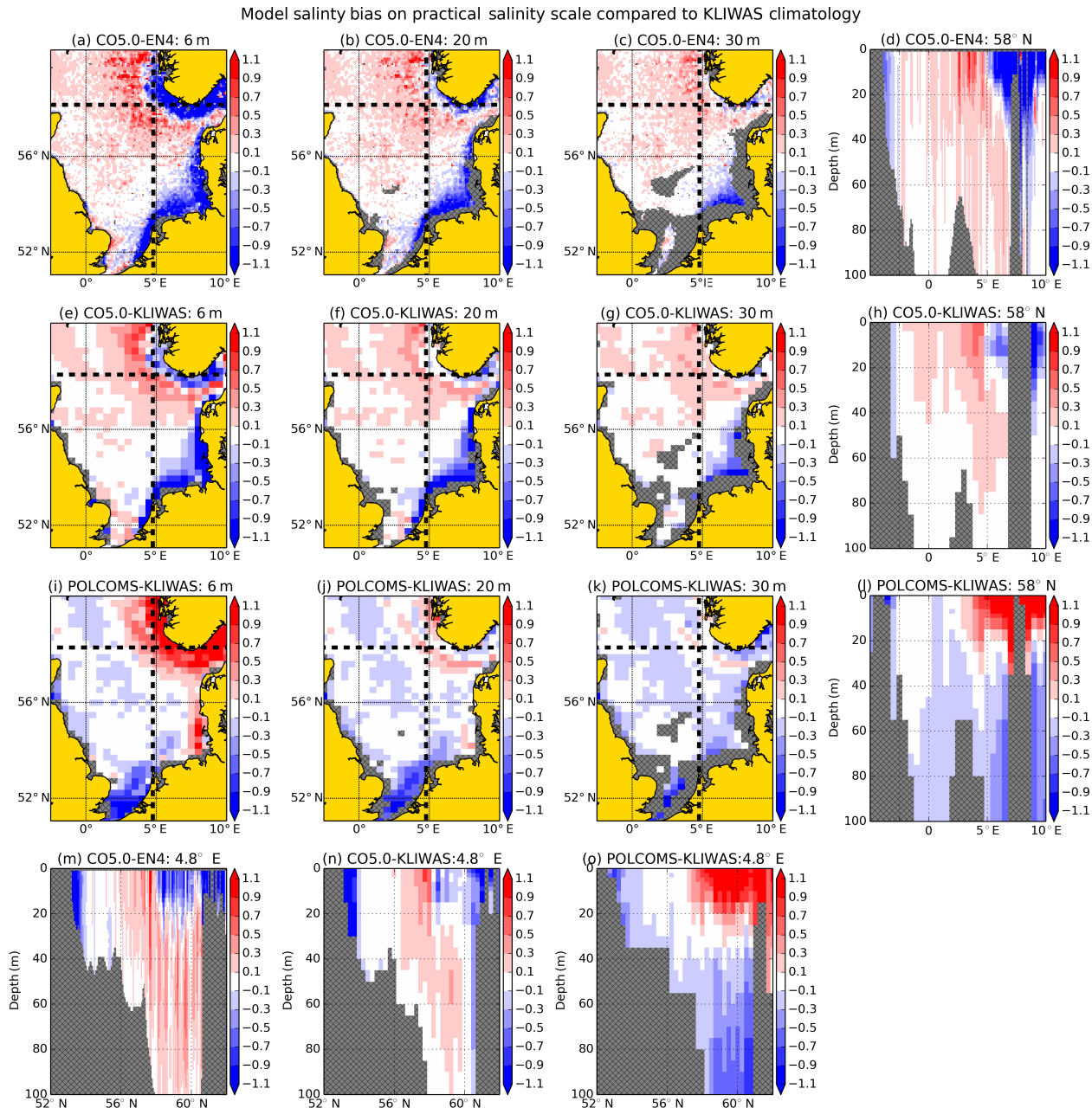
Figure 11. North Sea salinity bias compared to annual EN4 and KLIWAS climatology. Panels **(a)**–**(d)** compare CO5 and EN4 at 6, 20 and 30 m and along a transect at 58° N. Panels **(e)**–**(h)** compare CO5 and KLIWAS climatology at 6, 20 and 30 m and along a transect at 58° N. Panels **(e)**–**(h)** compare POLCOMS and KLIWAS climatology at 6, 20 and 30 m and along a transect at 58° N. Panels **(m)**–**(o)** are transects through depth for each case along longitude 4.8° E.

to the E-HYPE rivers resulting in an overall freshening compared to the climatologies.

5.3.3 Light attenuation

The summertime biases in temperature were shown to be significantly different between POLCOMS and CO5. Sensitivity experiment S30_5 explores replacing the light attenua-

tion scheme in CO5 with the PDWL scheme. Figure 15 compares the control experiment and experiment S30_5 over the summer. Figure 15a compares each run on shelf in regions of seasonal stratification. Using the PDWL light scheme has three effects: it increases the warm surface temperature bias, it increases the mid-depth cold bias and it reduces the bias from 40 m to the bed. The partition of solar radiation into a penetrating part and a non-penetrating part is dealt with dif-
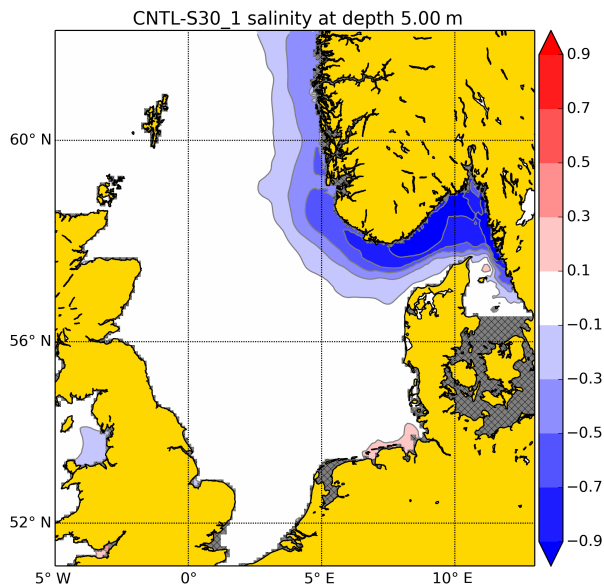
Figure 12. Comparison of mean salinity at 5 m between CO5 with 51 vertical levels using the Siddorn and Furner stretching function (CNTL) and 33 vertical levels using the Song and Haidvogel stretching function (S30_1). The hashed area in the Kattegat indicates the interface to Baltic NSBS model data.
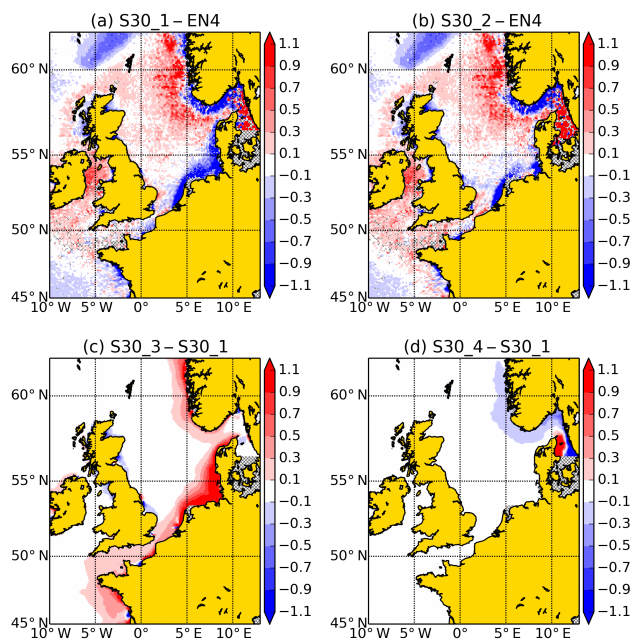

Figure 13. Comparing SSS using climatological river and Baltic inputs against E-HYPE rivers and IoW Baltic. Panel **(a)** shows 33 SH levels with E-HYPE rivers and IoW Baltic (S30_1) vs. EN4. Panel **(b)** shows 33 SH levels with climatological rivers and climatological Baltic (S30_2) vs. EN4. Panel **(c)** shows climatological rivers minus E-HYPE rivers (S30_3–S30_1). Panel **(d)** shows climatological Baltic – IoW Baltic (S30_4–S30_1).
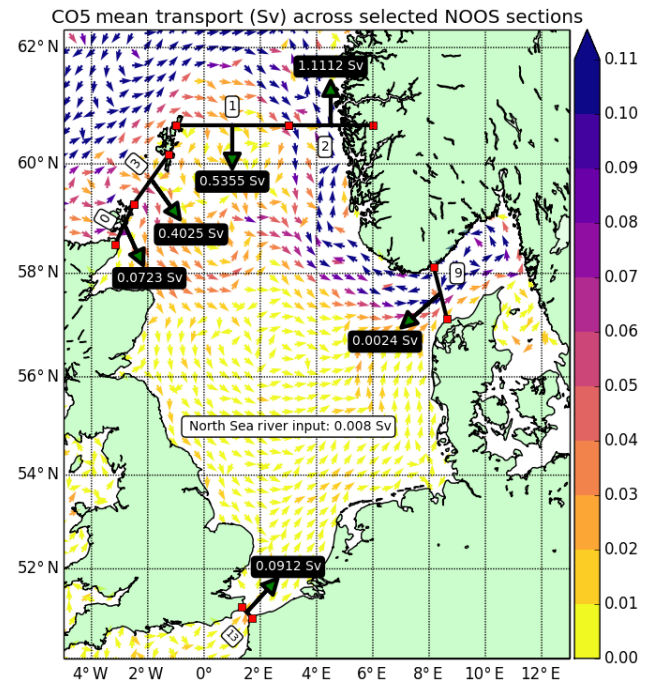
Figure 14. CO5 mean transport across selected NOOS transects surrounding the North Sea and the CO5 transport field shown only every fourth grid point for clarity.

ferently in each scheme and influences the degree of bias at the surface. In the PDWL scheme, all of the non-penetrating part is added to the surface layer, while in the RGB scheme there is still a slight penetration of the quickly attenuating light. The cold bias in both models indicates that the depth of the thermocline is too shallow, which could be either be due to the light not penetrating far enough in both schemes or insufficient vertical mixing. At depth, the PDWL scheme results in less heat being mixed down, resulting in a better agreement with the bed temperature as the RGB scheme is biased warm there. However, in mixed areas on shelf, both models appear to be too warm, which may indicate a bias in the surface flux forcing.

Figure 15b compares each scheme against the mean of the profiles off shelf south of 60° N. Figure 15b does not show depths below 140 m as the differences due to light below this depth are negligible. The large cold bias in the upper layers of the ocean north of 60° N biases the whole field cold. Thus, to obtain a better representation of the effect of the light scheme in the absence of large underlying biases, we restrict the mean to south of 60° N. As the light penetrates more deeply off shelf in the PDWL light scheme, the warm bias at the surface is less than the RGB scheme and the cold bias below 20 m is also reduced. Both schemes are similarly cold biased below 60 m where the direct effect of light penetration is small.
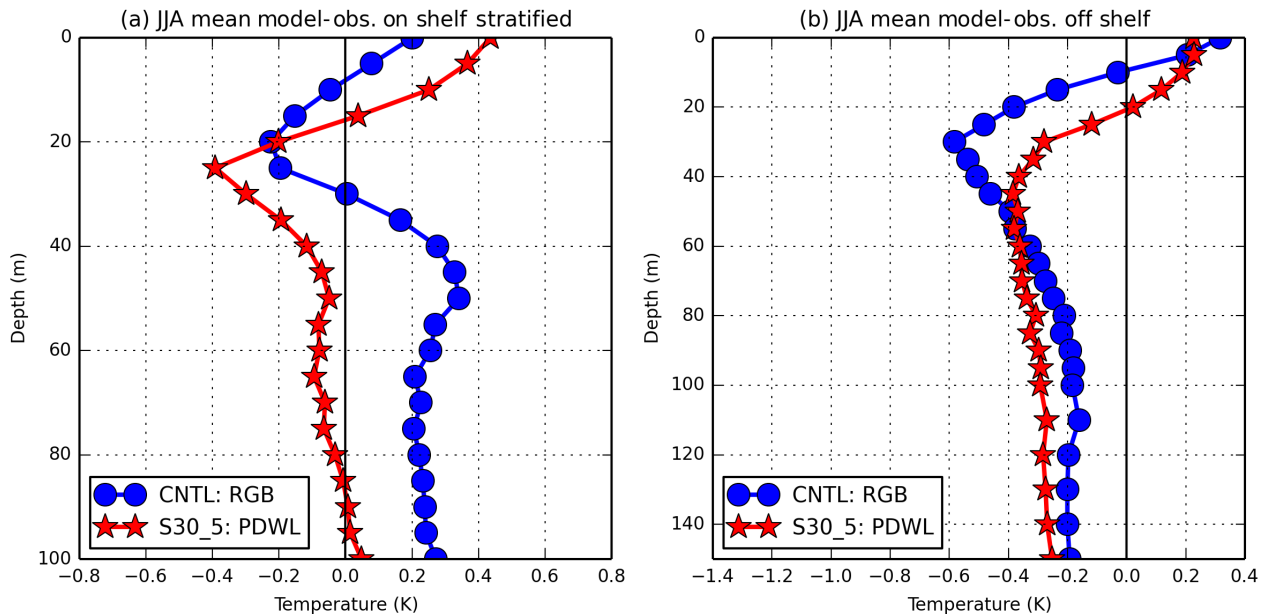
Figure 15. Comparison of summertime profiles compared to NEMO's three-band light attenuation scheme (RGB) and POLCOMS single-band scheme (PDWL). Panel **(a)** compares CNTL and S30_5 against the mean of profiles in the seasonally stratified part of the domain on shelf. Panel **(b)** compares CNTL and S30_5 against the mean of profiles off shelf south of 60° N.

5.4 The 5-year sensitivity runs

The shorter CO4 experiments of O'Dea et al. (2012) used different open ocean boundary conditions and surface boundary conditions relative to the CO5 control run. To further explore CO4 and CO5 differences whilst using the same forcing conditions of CO4, a set of sensitivity experiments for 5 years were undertaken starting in November 2006. The constraint on the start date is the availability of Met Office NWP flux data and the open boundary conditions used in CO4 which start from November 2006. All the 5-year experiments as detailed in Table 3 have 33 vertical levels with the Song and Haidvogel stretching function (Song and Haidvogel, 1994). They also use climatological rivers, climatological Baltic and the single-band light attenuation scheme implemented in CO4. The sensitivity of the model to the vertical coordinate, rivers, the Baltic boundary and the light attenuation scheme is explored in the 30-year experiments in Sect. 5.3. They are not shown to have significant impact on the large SST bias from Iceland to the Faroe Islands. In the following sections, the effects of changed boundaries and fluxes with an emphasis on the sensitivity of the SST bias to these changes is detailed.

5.4.1 Inverse barometer and open ocean boundary condition

The 5-year sensitivity experiments show that the most significant differences between CO4 and CO5 are related to the lateral boundary conditions. A bug in NEMO v3.2 prevented

the application of the inverse barometer effect on the open ocean lateral boundaries. Thus, two sensitivity experiments with NEMO v3.4 were conducted: S5_1 with this bug deliberately included and S5_2 without. An additional experiment, S5_3, is an equivalent experiment with exactly the same forcing but with NEMO v3.2 as the base model.

The resulting 5-year mean SST difference between S5_1 and S5_2 is shown in Fig. 16a. Clearly the switching on or off of the inverse barometer on the open boundary has a large impact on the SST in the north of the domain. The difference between the SST RMSE of S5_1 and S5_2 shown in Fig. 16d. The much larger RMSE of S5_1 indicates that the inclusion of the inverse barometer effect on the boundary considerably reduces the SST skill there. However, if the inverse barometer is not included on the boundaries, anomalous northward-flowing boundary jet currents result. Figure 16b and e are the equivalent mean and RMSE differences between S5_2 and S5_3, which are very similar to that of Fig. 16a and d. The difference (not shown) between S5_1 and S5_3 is much smaller. Thus, a large component of the difference between CO4 and CO5 is the difference in the application of the inverse barometer effect on the lateral boundary.
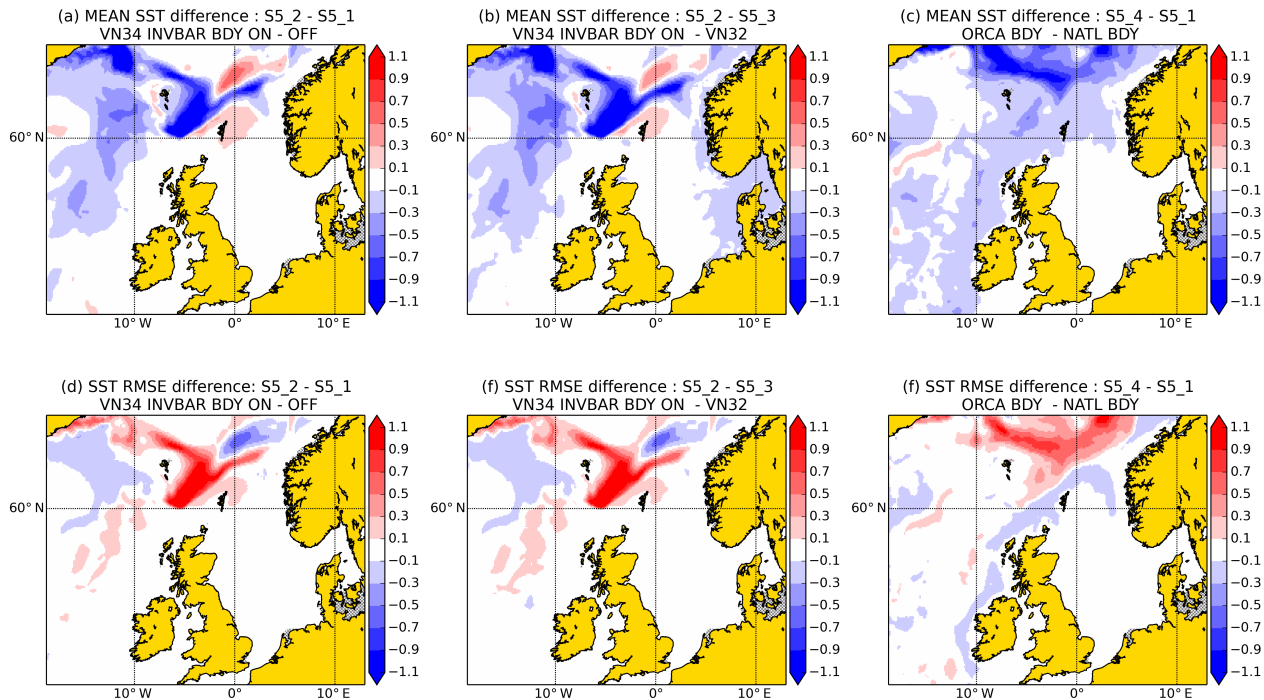
Figure 16. Isolating the difference in northern SST bias between CO4 and CO5. Panel **(a)** shows the mean SST difference between the NEMO v3.4 with the inverse barometer applied to the boundary and without (S5_2–S5_1). Panel **(b)** shows the mean SST difference between NEMO v3.4 with the inverse barometer applied to the boundary and NEMO v3.2 (S5_2–S5_3). Panel **(c)** shows the mean SST difference between NEMO v3.4 with ORCA025 and NATL12 boundary data (S5_4–S5_1). Panel **(d)** shows the difference between SST RMSE between NEMO v3.4 with the inverse barometer applied to the boundary and without (S5_2–S5_1). Panel **(e)** shows the difference between SST RMSE between the NEMO v3.4 with the inverse barometer applied to the boundary and NEMO v3.2 (S5_2–S5_3). Panel **(f)** shows the difference of SST RMSE between NEMO v3.4 with ORCA025 and NATL12 boundary data (S5_4–S5_1).

Another significant difference was the open ocean source data interpolated onto the open boundaries of CO5 and CO4. The 30-year sensitivity experiments of CO5 used data from the $1/4°$ global ocean domain (ORCA025). However, CO4 was forced using a $1/12°$ model of the North Atlantic (NATL12). In operational implementation of CO5, the higher resolution NATL12 model is also used to derive open boundaries. Sensitivity experiment S5_4 is exactly the same as S5_1 but replaces the ORCA025-derived boundaries with boundaries derived from the NATL12 model. The mean and RMSE SST differences between S5_1 and S5_4 are shown in Fig. 16c and f. The NATL12 data result in a warmer SST from Iceland to the Faroe Islands and a reduced RMSE compared to the ORCA025 data.

The GLOSEA5 surface data are compared against WOA13 in Fig. 17. Compared to WOA13, GLOSEA5 is anomalously cold and fresh along the CO5 boundary of $65°$ N. This suggests that a significant component of the northern bias in CO5 originates in the global model that provides its northern boundary condition.
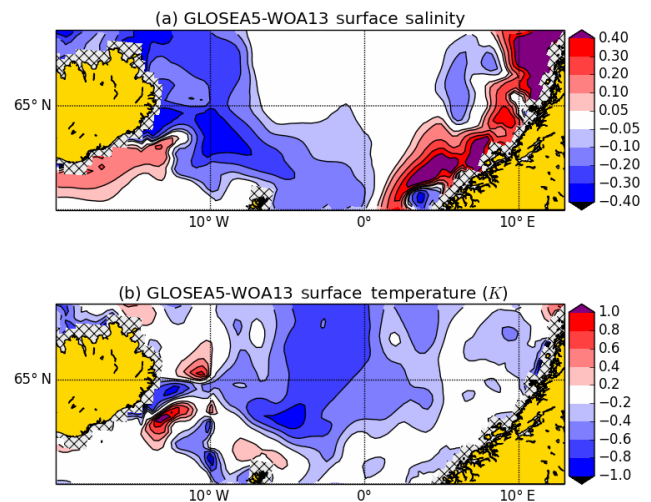

Figure 17. GLOSEA5 minus WOA13. Panel **(a)** is mean surface salinity. Panel **(b)** is the mean surface temperature.
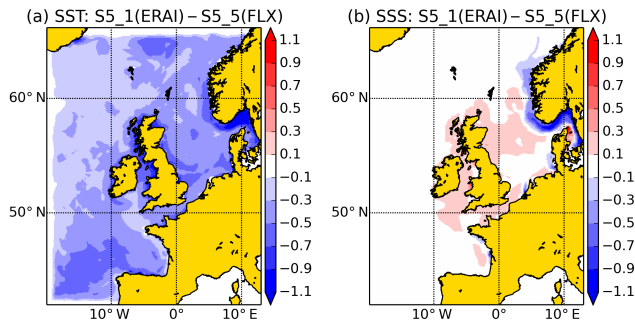
Figure 18. Comparison of mean SST **(a)** and SSS **(b)** differences between ERAI fluxes and NWP fluxes (S5_1 vs. S5_5).

5.4.2 Surface fluxes

Another important difference between CO4 and CO5 is the surface fluxes. In operational implementation, the surface fluxes are taken from the Met Office NWP model. The experiments in O'Dea et al. (2012) were also forced with NWP directly prescribed fluxes. However, comparable NWP model data were not available from before 2006, and thus the longer runs, as in the CO5 control, use ERAI surface fluxes. Furthermore, the NWP fluxes are directly prescribed in contrast to the CORE bulk formulae used with ERAI. A Haney correction (Haney, 1971) must also be applied when using direct fluxes with a prescribed reference SST as used by the NWP model itself.

Sensitivity experiment S5_5 is exactly as S5_1 but with ERAI-derived fluxes instead of NWP fluxes. Figure 18a and b compare the mean SST and SSS between S5_5 and S5_1. The SST is almost uniformly warmer with NWP fluxes than ERAI-derived fluxes, particularly in the Bay of Biscay, around the coast of the UK and into the Skagerrak and southern Norwegian Trench.

However, it should also be noted that because direct fluxes use the Haney correction, the resulting model SST is indirectly relaxed to the prescribed SST in a hindcast simulation. Furthermore, in NEMO version 3.2, the surface stress from direct fluxes was based on absolute wind velocity rather than wind velocity relative to the moving ocean surface. This has important localised effects in the vicinity of persistently strong surface currents, such as the Skagerrak. This sensitivity of the model to relative winds versus absolute winds using ERAI-derived forcing is also investigated. Figure 19 is the difference in the mean for 1 year of surface stress, salinity, current and temperature between using the relative wind velocity to the ocean surface and the absolute wind velocity.

Furthermore, the details of the fluxes near coastlines, and particularly the wind stress in the Skagerrak and southern Norwegian Trench, are quite different between the lower-resolution ERAI and higher-resolution NWP fluxes. The differing resolution of the surface forcing and the use of abso-
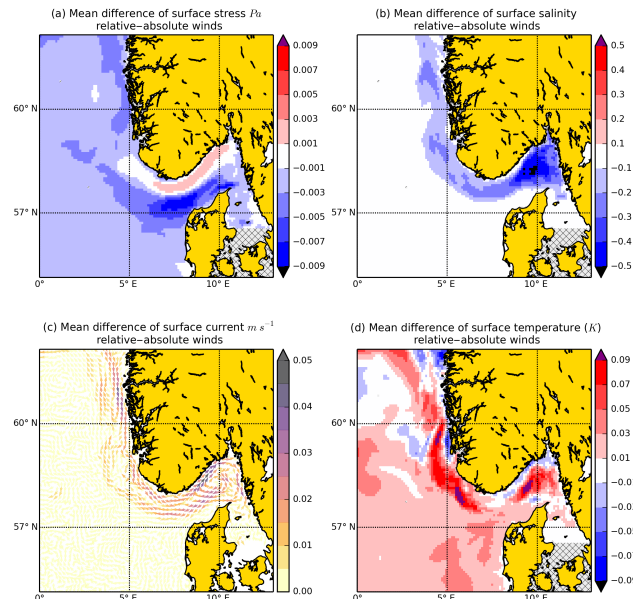

Figure 19. Comparison between using wind velocity relative to ocean surface and absolute wind velocity for the 2011 annual mean. Panel **(a)** shows the difference in surface shear stress in Pa. Panel **(b)** shows the difference in surface salinity. Panel **(c)** shows the difference in surface current. Panel **(d)** shows the difference in surface temperature.

lute instead of relative wind stress is thus likely to play a role in the different sensitivity experiments.

In Fig. 18b, it is shown that the experiment with ERAI-derived forcing is slightly more saline on shelf but significantly fresher in the Skagerrak and the Norwegian Trench mirroring the SST differences there. The difference in the shear stress modifies both the transport of the surface fresh layer out of the Skagerrak and the transport of relatively saline water from the North Sea into the Skagerrak. The difference in relative and absolute winds is significant also along the shelf break from the Shetland Islands northwards. In this case, the effect of using the absolute wind velocity is to reduce the transport of North Atlantic water northwards, which results in locally lower mean SST. With respect to the difference between ERAI-derived forcing and NWP-forced experiments, the difference in the SST in this local region is reduced. The reduction in the mean difference of SST is due to the countervailing effects of general domain-wide cold bias between ERAI-derived forcing and NWP fluxes, and the local cooling due to using absolute winds with the direct NWP fluxes.

6 Summary and discussion

The details of the standard coastal ocean model CO5 for the NWS were presented. CO5 was jointly developed by the Met Office and the National Oceanography Centre. This standard

model forms the basis of the physics component of the current CMEMS reanalysis of the NWS, which also includes data assimilation. CO5 is a regional tidal implementation of NEMO version 3.4, building upon CO4 (O'Dea et al., 2012) which used NEMO version 3.2 as the base code. In this paper, a 30-year physics-only control of CO5 using ERAI-derived surface forcing and ORCA025 lateral boundary conditions has been assessed against standard climatologies and observations to understand the impact of model physics on biases. The assessment compares CO5 to a POLCOMS-based hindcast over the period 1985–2004, which is a period covered by both hindcasts. A set of 30-year sensitivity hindcasts has also been assessed to understand several changes, relative to CO4, introduced into CO5. A further set of 5-year sensitivity experiments focusing on different surface and lateral boundary conditions has also been investigated.

Overall the CO5 tides are of comparable quality to CO4. The reference density of $1035 \, \text{kg} \, \text{m}^{-3}$ used in the control run slightly degraded the tidal predictions. The position of the degenerate amphidrome in southern Norway is slightly changed in CO5 mainly due to a small modification the land–sea mask originating from a change in the Baltic boundary condition.

Compared to AVHRR data, CO5 has a large SST bias extending from Iceland to the FSC. It is particularly pronounced in winter and partially obscured in summer due to surface heating. POLCOMS also has a large seasonal cold SST bias in the region but also a significant warm SST bias domain-wide in summer. In comparison to the AVHRR observations, CO5 appears to significantly improve upon the simulation of SST in the POLCOMS hindcast.

As in the SST, CO5 has a similar pattern of fresh bias in the near-surface salinity from Iceland to the FSC as well as a large fresh bias in the German Bight due to E-HYPE rivers and a dipole of surface salinity bias along the Norwegian Trench that suggests insufficient lateral mixing. POLCOMS, in contrast, is slightly too saline in the German Bight and uniformly too saline at the surface along the Norwegian Trench.

Both CO5 and POLCOMS appear to lose the identity of relatively warm saline Mediterranean water near the southern boundary of the domain. In CO5, there is a sponge layer in the boundary relaxation zone where the diffusion is increased for model stability. Furthermore, the vertical resolution is focused on the surface and bed and is particularly coarse mid-water in the deeper parts of the domain. Both of these may be contributing to the apparent overestimation of diffusion of this water mass both laterally and vertically.

In the North Sea, there is a marked difference in the vertical summer temperature profile between POLCOMS and CO5 in seasonally stratified regions. Compared to climatology and observations, POLCOMS is much too warm at the surface, while both POLCOMS and CO5 are too cold mid-water, and CO5 is too warm towards the bed.

The single-band light scheme (PDWL) used in POL-COMS and CO4 was seen to significantly alter the temperature profile in seasonally stratified regions in CO5. Introducing the PDWL scheme into CO5 leads to a larger warm bias at the surface and a larger colder mid-water cold bias than the CO5 control. From 40 m to the bed, the PDWL light attenuation scheme resulted in closer agreement with climatology than the CO5 control run. Both models appear to be over-stratifying with a very abrupt thermocline. Whilst the light attenuation scheme may be a component of this error, the vertical mixing will also be an important contributor and should be a subject of further refinement.

The sensitivity experiments also explored the significance of changing the riverine inputs and the Baltic boundary condition. The older climatological rivers greatly reduce the freshwater bias in the German Bight and also near the Norwegian coast. It appears that the version of E-HYPE used in CO5 has too much freshwater discharge from continental Europe. The Baltic boundary condition used in CO5 results in slightly more saline surface waters in the Norwegian Trench. The added variability introduced by the CO5 Baltic boundary relative to the CO4 climatological boundary cannot be assessed by the long-term climatological means used in this paper. Further site-specific studies in the Kattegat and Skagerrak are required to evaluate the variability.

The impact of the change in vertical levels has a significant impact on the mean surface salinity in the Norwegian Trench. The increase in surface resolution allows retention of the relatively fresh layer of Baltic origin more than the coarser vertical levels used in CO4.

The 5-year sensitivity experiments revealed that a bug fix in CO5 related to the application of the inverse barometer effect on the lateral boundaries results in a colder SST from Iceland to the FSC. This is the region where CO5 has a particularly large SST cold bias and partially explains why CO5 has larger SST errors here than CO4. The inclusion of the inverse barometer effect on the boundaries results in a greater transport of water southwards from the northern boundary and with it colder fresher water. The source data for the boundaries themselves also have a significant impact in this region. The higher resolution 1/12° NATL12 model results in smaller cold bias there also. It is likely that 1/4° ORCA025 global model lacks sufficient resolution to model the Icelandic shelf in the vicinity of the northern CO5 boundary. The increased southwards transport of water from the northern boundary condition due to the inclusion of the inverse barometer effect amplifies the cold and fresh anomaly of the ORCA025 boundary data.

The impact of changing the surface boundary conditions from ERAI and CORE bulk forcing and directly specified fluxes from the Met Office NWP model was also investigated. The NWP fluxes as used in CO4 resulted in a warmer mean SST, further offsetting the generally cold bias in the CO5 control off shelf. However, it also led to a slight mean warm bias on shelf, with the exception of the Skagerrak where the fluxes have a fairly large cold bias. The direct fluxes as applied in CO4 used the absolute wind velocity

rather than the relative wind velocity compared to the moving ocean surface. The effect of using relative versus absolute wind velocities has important impacts in localised regions with persistent strong surface currents such as the Skagerrak. The ERAI-derived forcing is also of a relatively coarse resolution and the details of near-coastal fluxes are quiet different from the NWP fluxes. The combined difference of absolute versus relative winds and differing details in the fluxes combine to have significant impacts on surface transport and hence surface salinity in local regions such as the Skagerrak.

In summary, CO5 has been shown to produce a significantly improved hindcast of the NWS compared to POLCOMS against climatologies and observations. However, there are a number of notable biases in CO5 that need addressing in future configurations. Particular issues relate to freshwater inputs from rivers, surface boundary conditions as well as seasonal stratification in the North Sea.

The next standard configuration CO6 will be an incremental update for the physics based on some of the lessons learned from CO5. The relative stability of physics developments between CO5 and CO6 allows for significant updates to both data assimilation and biology components for the NWS forecast system. Physics changes will include updating the base version of NEMO to 3.6, updating the light attenuation to use satellite-observed climatology of ocean colour instead of a domain-wide coefficient. The river inputs will be from an updated climatology with reduced biases compared to the E-HYPE rivers used in CO5. However, a step change in the physics will occur in CO7 when the resolution will be increased from 7 to 1.5 km. CO7 will be of a sufficient resolution to resolve the internal Rossby radius on the shelf. Possible improvements include capturing to first order the generation of internal tides at the shelf break, resolving mesoscale eddies and consequently enhanced mixing in the Norwegian Trench and greatly improving bathymetry and coastline to name but a few. Furthermore, CO7 is being developed in anticipation of the longer-term goals of coupling to wave, atmosphere and land system models. The aspiration is to drive towards eventual operational coupled implementation for which CO7 will form the basis of the ocean model component.

Appendix A: FPP keys used in CO5

Table A1. FPP keys used with the CO5 control experiment.

key_tide	Activate tidal potential forcing
key_dynspg_ts	Free surface volume with time splitting
key_ldfslp	Rotation of lateral mixing tensor
key_iomput	Input output manager
key_vvl	Variable volume layer
key_shelf	Diagnostic switch for output
key_zdfgls	Generic length-scale turbulence scheme
key_bdy	Use open lateral boundaries
key_amm	Dimensions for AMM domain
key_levels=51	Number of vertical levels

Appendix B: Adjusting the lateral open ocean boundary conditions

The lateral open ocean boundary conditions are derived from three separate 1/4° ORCA025 experiments. The years 1981 to 1989 are also taken from the GO5.0 1/4° ORCA025 hindcast (Megann et al., 2014). The boundary conditions from 1989 onwards are taken from the two separate Global Seasonal Forecast system version 5 (GLOSEA5) (MacLachlan et al., 2015) experiments spanning 1989–2003 and 2003–2012.

Each of ORCA025 experiments had substantially different mean SSH. They needed to be matched at the cross-over dates as closely as possible to prevent large shocks. The free-running model GO5 experiment for the 1980s was shown to have a long-term unrealistic drift in the mean SSH. This long-term trend is removed from the data before deriving boundary conditions. Furthermore, the first GLOSEA run does not have altimeter assimilation until 1992 and likewise has an unrealistic drift removed from these initial years (1989–1992).

Once the data are detrended, a mean SSH is calculated area wide at the cross-over dates in 1989 and 2003. The second GLOSEA dataset is taken as the reference. The difference in the mean SSH in the earlier detrended GO5.0 experiment at the 1989 crossover data is then subtracted from the entire period (1981–1989). This, in effect, is a uniform shift in SSH so that at the cross-over date the discrepancy is as reduced as possible. Similarly, the difference in the mean between the first GLOSEA run and the second is used to match the two in 2003. However, even after this prepossessing, there is still some transient adjustment in SSH, particularly so at the 2003 cross-over.

Appendix C: Other inputs

The bathymetry used in CO5 is made publicly available from https://doi.org/10.13140/RG.2.2.25799.50081 (O'Dea, 2016a).

References

Arakawa, A. and Lamb, V. R.: A potential enstrophy and energy conserving scheme for the shallow water equations, Mon. Weather Rev., 109, 18–36, 1981.

Bersch, M., Gouretski, V., Sadikni, R., and Hinrichs, I.: KLIWAS North Sea Climatology of Hydrographic Data (Version 1.0), Tech. rep., Center for Earth System Research and Sustainability (CEN), University of Hamburg, https://doi.org/10.1594/WDCC/KNSC_hyd_v1.0, 2013.

Canuto, V., Howard, A., Cheng, Y., and Dubovikov, M.: Ocean turbulence. Part I: One-point closure model-momentum and heat vertical diffusivities, J/ Phys/ Oceanogr., 31, 1413–1426, 2001.

Casey, K. S., Brandon, T. B., Cornillon, P., and Evans, R.: The Past, Present, and Future of the AVHRR Pathfinder SST Program, Springer Netherlands, Dordrecht, 273–287, https://doi.org/10.1007/978-90-481-8681-5_16, 2010.

Craig, P. D. and Banner, M. L.: Modeling wave-enhanced turbulence in the ocean surface layer, J. Phys. Oceanogr., 24, 2546–2559, 1994.

Dee, D., Uppala, S., Simmons, A. et al.: The ERA-Interim reanalysis: Configuration and performance of the data assimilation system, Q. J. Roy. Meteorol. Soc., 137, 553–597, 2011.

Donnelly, C., Andersson, J. C., and Arheimer, B.: Using flow signatures and catchment similarities to evaluate the E-HYPE multi-basin model across Europe, Hydrol. Sci. J., 61, 255–273, https://doi.org/10.1080/02626667.2015.1027710, 2015.

Galperin, B., Kantha, L., Hassid, S., and Rosati, A.: A quasi-equilibrium turbulent energy model for geophysical flows, J. Atmos. Sci., 45, 55–62, 1988.

Good, S. A., Martin, M. J., and Rayner, N. A.: EN4: Quality controlled ocean temperature and salinity profiles and monthly objective analyses with uncertainty estimates, J. Geophys. Res.-Oceans, 118, 6704–6716, https://doi.org/10.1002/2013JC009067, 2013.

Gräwe, U., Holtermann, P., Klingbeil, K., and Burchard, H.: Advantages of vertically adaptive coordinates in numerical

models of stratified shelf seas, Ocean Model., 92, 56–68, https://doi.org/10.1016/j.ocemod.2015.05.008, 2015.

Haney, R. L.: Surface thermal boundary condition for ocean circulation models, J. Phys. Oceanogr., 1, 241–248, 1971.

Holt, J. and Proctor, R.: The seasonal circulation and volume transport on the northwest European continental shelf: A fine-resolution model study, J. Geophys. Res.-Oceans, 113, https://doi.org/10.1029/2006JC004034, 2008.

Holt, J., Hughes, S., Hopkins, J., Wakelin, S. L., Holliday, N. P., Dye, S., González-Pola, C., Hjøllo, S. S., Mork, K. A., Nolan, G., Proctor, R., Read, J., Shammon, T., Sherwin, T., Smyth, T., Tattersall, G., Ward, B., and Wiltshire, K. H.: Multi-decadal variability and trends in the temperature of the northwest European continental shelf: A model-data synthesis, Prog. Oceanogr., 106, 96–117, https://doi.org/10.1016/j.pocean.2012.08.001, 2012.

Holt, J. T. and James, I. D.: An s coordinate density evolving model of the northwest European continental shelf: 1. Model description and density structure, J. Geophys. Res.-Oceans, 106, 14015–14034, https://doi.org/10.1029/2000JC000304, 2001.

Howarth, M. and Pugh, D.: Chapter 4 Observations of Tides Over the Continental Shelf of North-West Europe, Elsevier Oceanography Series, 35, 135–188, https://doi.org/10.1016/S0422-9894(08)70502-6, 1983.

Ingleby, B. and Huddleston, M.: Quality control of ocean temperature and salinity profiles – Historical and real-time data, J. Marine Syst., 65, 158–175, https://doi.org/10.1016/j.jmarsys.2005.11.019, 2007.

Large, W. and Yeager, S.: The global climatology of an interannually varying air–sea flux data set, Clim. Dynam., 33, 341–364, 2009.

Lawrence, B. N., Bennett, V. L., Churchill, J., Juckes, M., Kershaw, P., Pascoe, S., Pepler, S., Pritchard, M., and Stephens, A.: Storing and manipulating environmental big data with JASMIN, in: 2013 IEEE International Conference on Big Data, 68–75, https://doi.org/10.1109/BigData.2013.6691556, 2013.

Lengaigne, M., Menkes, C., Aumont, O., Gorgues, T., Bopp, L., André, J.-M., and Madec, G.: Influence of the oceanic biology on the tropical Pacific climate in a coupled general circulation model, Clim. Dynam., 28, 503–516, https://doi.org/10.1007/s00382-006-0200-2, 2007.

Levier, B., Tréguier, A. M., Madec, G., and Garnier, V.: Free surface and variable volume in the NEMO code, MESRSEA IP report WP09-CNRS-STR03-1A, 2007.

Lindström, G., Pers, C., Rosberg, J., Strömqvist, J., and Arheimer, B.: Development and testing of the HYPE (Hydrological Predictions for the Environment) water quality model for different spatial scales, Hydrol. Res., 41, 295–319, https://doi.org/10.2166/nh.2010.007, 2010.

MacLachlan, C., Arribas, A., Peterson, K. A., Maidens, A., Fereday, D., Scaife, A. A., Gordon, M., Vellinga, M., Williams, A., Comer, R. E., Camp, J., Xavier, P., and Madec, G.: Global Seasonal forecast system version 5 (GloSea5): a high-resolution seasonal forecast system, Q. J. Roy. Meteor. Soc., 141, 1072–1084, https://doi.org/10.1002/qj.2396, 2015.

Madec, G.: NEMO ocean engine: Note Du Pôle de Modél, Institut Pierre-Simon Laplace (IPSL), France, No 27, 2008.

Megann, A., Storkey, D., Aksenov, Y., Alderson, S., Calvert, D., Graham, T., Hyder, P., Siddorn, J., and Sinha, B.: GO5.0: the joint NERC–Met Office NEMO global ocean model for use in

coupled and forced applications, Geosci. Model Dev., 7, 1069–1092, https://doi.org/10.5194/gmd-7-1069-2014, 2014.

Merchant, C. J., Embury, O., Roberts-Jones, J., Fiedler, E., Bulgin, C. E., Corlett, G. K., Good, S., McLaren, A., Rayner, N., Morak-Bozzo, S., and Donlon, C.: Sea surface temperature datasets for climate applications from Phase 1 of the European Space Agency Climate Change Initiative (SST CCI), Geoscience Data Journal, 1, 179–191, https://doi.org/10.1002/gdj3.20, 2014.

O'Dea, E.: CO5 Bathymetry, https://doi.org/10.13140/RG.2.2.25799.50081, 2016a.

O'Dea, E.: CO5 AMM7 namelist, https://doi.org/10.13140/RG.2.2.17410.89286, 2016b.

O'Dea, E. J., Arnold, A. K., Edwards, K. P., Furner, R., Hyder, P., Martin, M. J., Siddorn, J. R., Storkey, D., While, J., Holt, J. T., and Liu, H.: An operational ocean forecast system incorporating NEMO and SST data assimilation for the tidally driven European North-West shelf, Journal of Operational Oceanography, 5, 3–17, 2012.

Otto, L., Zimmerman, J., Furnes, G., Mork, M., Saetre, R., and Becker, G.: Review of the physical oceanography of the North Sea, Neth. J. Sea Res., 26, 161–238, https://doi.org/10.1016/0077-7579(90)90091-T, 1990.

Prandle, D., Ballard, G., Flatt, D., Harrison, A., Jones, S., Knight, P., Loch, S., McManus, J., Player, R., and Tappin, A.: Combining modelling and monitoring to determine fluxes of water, dissolved and particulate metals through the Dover Strait, Cont. Shelf Res., 16, 237–257, https://doi.org/10.1016/0278-4343(95)00009-P, 1996.

Rodi, W.: Examples of calculation methods for flow and mixing in stratified fluids, J. Geophys. Res.-Oceans, 92, 5305–5328, 1987.

Siddorn, J. and Furner, R.: An analytical stretching function that combines the best attributes of geopotential and terrain-following vertical coordinates, Ocean Model., 66, 1–13, 2013.

Sikirić, M. D., Roland, A., Janeković, I., Tomazˇić, I., and Kuzmić, M.: Coupling of the Regional Ocean Modeling System (ROMS) and Wind Wave Model, Ocean Model., 72, 59–73, https://doi.org/10.1016/j.ocemod.2013.08.002, 2013.

Song, Y. and Haidvogel, D.: A Semi-implicit Ocean Circulation Model Using a Generalized Topography-following Coordinate System, J. Comput. Phys., 115, 228–244, https://doi.org/10.1006/jcph.1994.1189, 1994.

Tinker, J., Lowe, J., Holt, J., Pardaens, A., and Wiltshire, A.: Validation of an ensemble modelling system for climate projections for the northwest European shelf seas, Prog. Oceanogr., 138, 211–237, https://doi.org/10.1016/j.pocean.2015.07.002, 2015.

Umlauf, L. and Burchard, H.: A generic length-scale equation for geophysical turbulence models, J. Marine Res., 61, 235–265, 2003.

Umlauf, L. and Burchard, H.: Second-order turbulence closure models for geophysical boundary layers. A review of recent work, Cont. Shelf Res., 25, 795–827, 2005.

Young, E. and Holt, J.: Prediction and analysis of long-term variability of temperature and salinity in the Irish Sea, J. Geophys. Res.-Oceans, 112, https://doi.org/10.1029/2005JC003386, 2007.

Zalesak, S. T.: Fully multidimensional flux-corrected transport algorithms for fluids, J. Comput. Phys., 31, 335–362, 1979.

Zweng, M., Reagan, J., Antonov, J., Locarnini, R., Mishonov, A., Boyer, T., Garcia, H., Baranova, O., Johnson, D., Seidov, D., and Biddle, M.: World Ocean Atlas 2013, Volume 2: Salinity, Tech. Rep. NOAA Atlas NESDIS 74, NOAA, Silver Springs, MD, available at: http://http://data.nodc.noaa.gov/woa/WOA13/DOC/woa13_vol2.pdf (last access: 28 July 2017), 2013.